Integrated Environmental Assessment and Management — Volume 2, Number 3—p. 262–272

Original Research

Sediment Trend Analysis of the Hylebos Waterway: Implications for Liability Allocations

Patrick McLaren† and R Paul Beveridge‡*

†GeoSea® Consulting (Canada), 7236 Peden Lane, Brentwood Bay, British Columbia V8M 1C5
‡Heller Ehrman LLP, 701 Fifth Avenue, Suite 6100, Seattle, Washington 98104-7098, USA

(Received 29 September 2005; Accepted 4 October 2005)

EDITOR'S NOTE:

Additional supporting data are found in appendices available in the online edition of IEAM Volume (2), Number (3). DOI: 10.1897/2005-035.1.

ABSTRACT

Sediment trend analysis (STA) is a technique that determines the net patterns of sediment movement and their dynamic behavior or stability. The data required are the complete particle size distributions obtained from bottom grab samples collected in a regular grid over the area of interest. Appendix 1 provides the particular details of how STA is undertaken. Because many contaminants are known to associate with the natural particles contained in sedimentary deposits, STA can provide additional weight-of-evidence in ecological risk assessment, remedial investigation, remediation itself, and litigation issues. The STA was applied to 242 sediment samples collected from the Hylebos Waterway, Tacoma, Washington, USA, in support of remedial action planning, contaminant source identification, and ultimately allocation of legal liability for contamination. The Waterway itself comprises a narrow shipping channel extending 3 miles from Commencement Bay (Puget Sound) where it ends in a dredged turning basin (Upper Turning Basin). A 2nd dredged turning basin (Lower Turning Basin) is located about three-quarters of the distance down its length. Both sides of the channel are home to an extensive industrial complex associated with significant contaminant releases into the water. The area was declared a Superfund Site in the early 1980s.The results of the STA showed a consistent pattern of sediment transport directed from the mouth of the Waterway to the turning basin at its head. Divided into 5 separate transport environments (TEs), the sediments within the Waterway progress from transport in Dynamic Equilibrium near the mouth, to Total Deposition (type 1) in the vicinity of the Lower Turning Basin, followed by Total Deposition (type 2) in the Upper Turning Basin. Assuming that contaminants associate preferentially with the finer, rather than the coarser, components of the grain size distributions, a probable behavior of contaminants that can be contained in the sediments is proposed for each TE. Maps showing the spatial distributions of existing contaminant data appear to conform very well to the patterns that might be expected from the STA results. This evidence was primarily used to demonstrate that potentially responsible parties (PRPs) located at the head of the Waterway could not be responsible for contaminated sediments toward its mouth. The findings, for example, effectively dismissed the assumption by the Natural Resource Damage Trustee agencies that contaminated sediments from a particular source would be as likely to migrate down the Waterway as up the Waterway. As a result, major documented sources of contamination near the mouth should be expected to bear a larger share of the total cleanup compared with sources farther toward the head. Furthermore, the STA provided explanations for apparent anomalies such as how hot spots of polychlorinated biphenyls (PCBs) could be located near a property where PCBs had never been released into the environment. If sediment gradient pattern analysis alone were used to allocate liability among PRPs, those located near such hot spots would receive a disproportionate share of liability.

Keywords: Sediment Transport Contaminants Litigation

INTRODUCTION

Contaminated sediments do not always remain in place in the environment. The mobility of sediments and the particle-associated contaminants contained within them are a complicating factor in ecological risk assessment, remedial investigation, remediation itself, or ultimately in litigation. Rational decision making must take into account the probable stability of contaminated sediments, their sources, transport, and ultimate fate (e.g., US Environmental Protection Agency [USEPA] 2002; Apitz et al. 2005).

One technique that might help provide such information is sediment trend analysis (STA), an empirical method that examines relative changes in the complete grain size distributions of aquatic sediments to determine their net transport pathways together with their dynamic behavior (i.e., accretion, erosion, dynamic equilibrium). Because many contaminants adsorb onto the particles that make up natural sediment, this information can aid in assessing the relationship between contaminant loadings and their sources, as well as provide an understanding of the fate and behavior of contaminants contained in the sediments.

To support remedial action planning, source identification, and ultimately allocation of legal liability for contamination, STA was performed on 242 surficial sediment samples collected in July 2001 from the Hylebos Waterway in Tacoma, Washington, USA (Figure 1). The purposes of the study were principally to identify individual sediment transport environments on the basis of sediment characteristics and

* To whom correspondence may be addressed patrick@geosea.ca

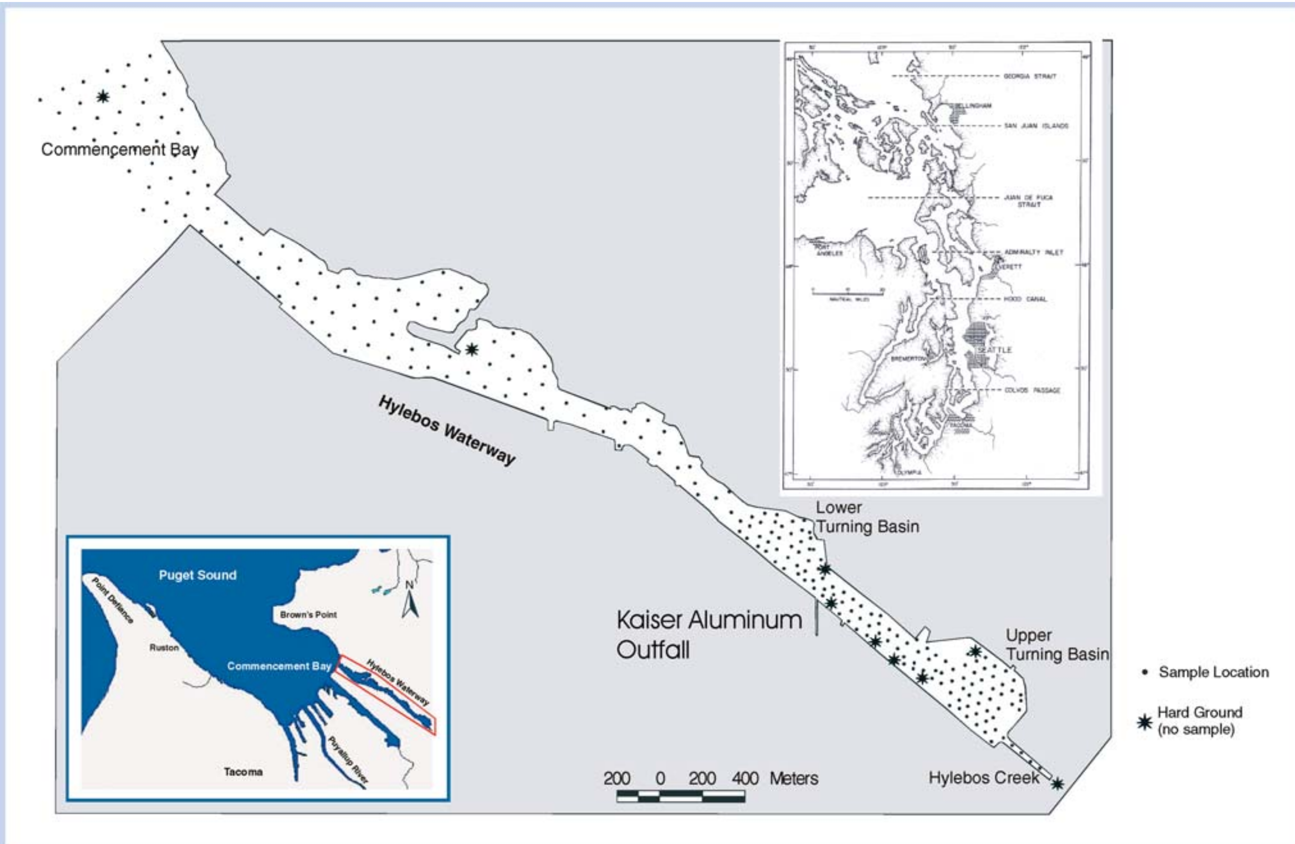

Figure 1. Sample sites and place names.

their dynamic behavior and to assess the probable extent of contamination from specific sources.

SEDIMENT TREND ANALYSIS

The theory to predict the relative changes that will occur in particle size distributions of sediments through erosion, transport, and deposition was 1st presented in McLaren and Bowles (1985). On the basis of their theory, several methods to carry out STA have been developed. The McLaren and Bowles approach is 1 dimensional, whereby the changes in grain size distributions along individual sample sequences are tested for validity with the Z score statistic to determine the preferred transport direction. A practical assessment of this approach is discussed in Hughes (2005). Gao and Collins (1991, 1992) and Gao (1996) proposed a 2-dimensional vector approach to determine trends, some elements of which were revised by Chang et al. (2001). A different vector approach altogether was produced by Le Roux (1994) and Le Roux et al. (2002). A summary of the various techniques is provided in Rios et al. (2003).

Regardless of the technique used to derive sediment trends, the original theory of how grain size distributions should change with transport has remained undisputed since the 1985 paper by McLaren and Bowles. Briefly, the theory demonstrated that, when 2 sediment samples (d_1 and d_2) are taken sequentially in a known transport direction (e.g., from a riverbed, where d_1 is the up-current sample and d_2 is the down-current sample), the sediment distribution of d_2 can become finer (case B) or coarser (case C) than d_1; if it becomes finer, the skewness of the distribution must become more negative. Conversely, if d_2 is coarser than d_1, the skewness must become more positive. The sorting will become better (i.e., the value for variance will become less) for both cases B and C. If either of these 2 trends is observed, sediment transport from d_1 to d_2 can be inferred. If the trend is different from the 2 acceptable trends (e.g., if d_2 is finer, better sorted, and more positively skewed than d_1), the trend is unacceptable and it cannot be supposed that transport between the 2 samples has taken place.

In the above example in which the transport direction is unequivocally known, $d_2(s)$ can be related to $d_1(s)$ by a function $X(s)$, where s is the grain size. The distribution of $X(s)$ can be determined by

$$X(s) = d_2(s)/d_1(s)$$

where $X(s)$ provides the statistical relationship between the 2 deposits and its distribution defines the relative probability of each particular grain size being eroded, transported, and deposited from d_1 to d_2. It is the shape of the $X(s)$ distribution relative to the shapes of the $d_1(s)$ and $d_2(s)$ distributions that determines the dynamic behavior (stability) of the sediments. The 5 defined categories for dynamic behavior are 1) Net Erosion, 2) Net Accretion, 3) Dynamic Equilibrium, 4) Total Deposition (type 1), and 5) Total Deposition (type 2). Appendix 1 (see Figure A6) contains a more thorough analysis of the theory and the procedures used in the derivation of the transport pathways.

METHODOLOGY

Sediment grab samples were collected from the Hylebos Waterway during the period 12–15 July 2001 with a Van Veen–type grab sampler. This device samples the top 10 to 15

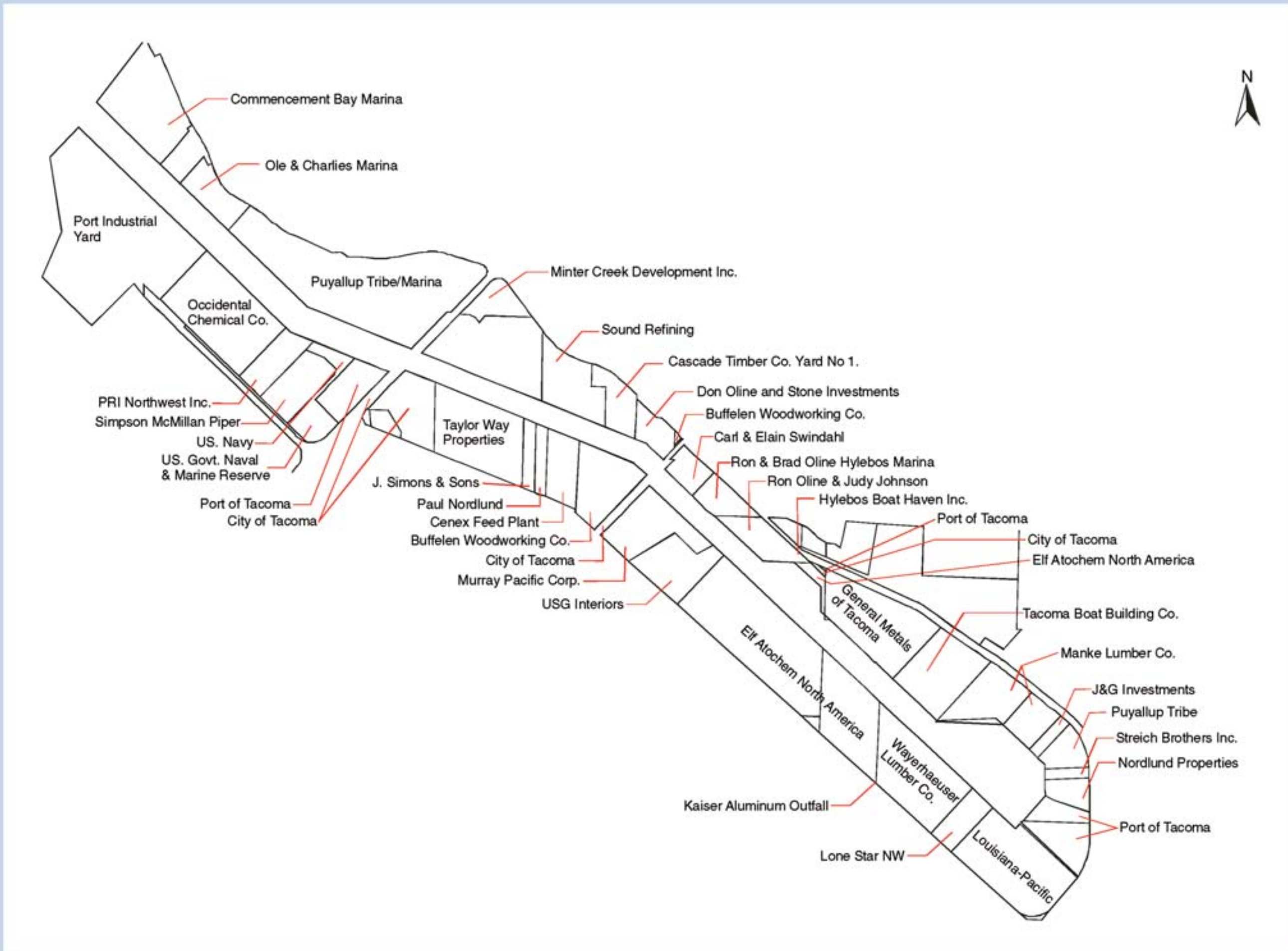

Figure 2. Industrial properties on the Hylebos Waterway.

cm of sediment, from which a mixed sample of 200 to 300 g encompassing the full depth of the sampler was obtained. As discussed in Appendix 1, the mixed sample is assumed to represent an average of all the sediment derived from an unknown number of sources or directions. All samples were collected from a 12-foot (3.7-m), hard-bottom inflatable speedboat equipped with a depth sounder, a small electric winch, and a grab sampler. Positions were obtained with a differential Global Positioning System receiver with 2-m accuracy in differential mode (Trimble DS212L). In most instances, samples were obtained at predetermined locations; however, where shoreline structures (e.g., docks and marinas) and vessels interfered with navigation, samples were collected as close as practicable to the planned position. Each sample was stored in a plastic zip-lock bag and transported to the GeoSea laboratory in Brentwood Bay, British Columbia, Canada, for grain size analysis.

Samples were collected on a regular hexagonal grid with a spacing of 110 m in the outer portion of the Waterway (from Commencement Bay to the start of the Lower Turning Basin) and 55 m to include the Lower Turning Basin landward to the Upper Turning Basin (Figure 1). A total of 251 sample sites were visited, of which 9 were found to be hard ground (usually occurring when bark mulch covered the bottom) and no sample could be taken. A site was designated "hard ground" after 3 separate drops of the grab sampler failed to retrieve sediment.

All samples were analyzed for their complete grain size distribution (range 1,800–1 μm) with a Malvern MasterSizer 2000 laser particle sizer. The laser-derived distributions were combined with sieve data for grain sizes of more than 1,500 μm by a merging algorithm. The distributions were entered into a computer equipped with appropriate software to establish sediment trends and transport functions.

PHYSICAL SETTING

The Hylebos is the northernmost of several man-made waterways that make up the industrial port facilities of the Tacoma Tideflats. Extending from Commencement Bay, it runs southeast for about 5 km and is generally about 200 m across. A small creek (Hylebos Creek) enters the Waterway at its extreme southeast end. The waterways themselves are constructed in old channels of the former Puyallup River delta, which now flows into Commencement Bay through the Puyallup Waterway. Although considerably changed by 20th century industrialization, the river still carries an active sediment load that is presently forming a delta at its mouth in Commencement Bay. Its suspended load is quite clearly visible in the Bay and, at the time of sampling, was seen to extend far into the Hylebos Waterway. Drogue studies in the Waterway have shown a net inflow of saline water below 6 m and a net outflow at 2 to 6 m. The surface also displays a net inflow, although wind from the southeast can reverse this (Loehr et al. 1981).

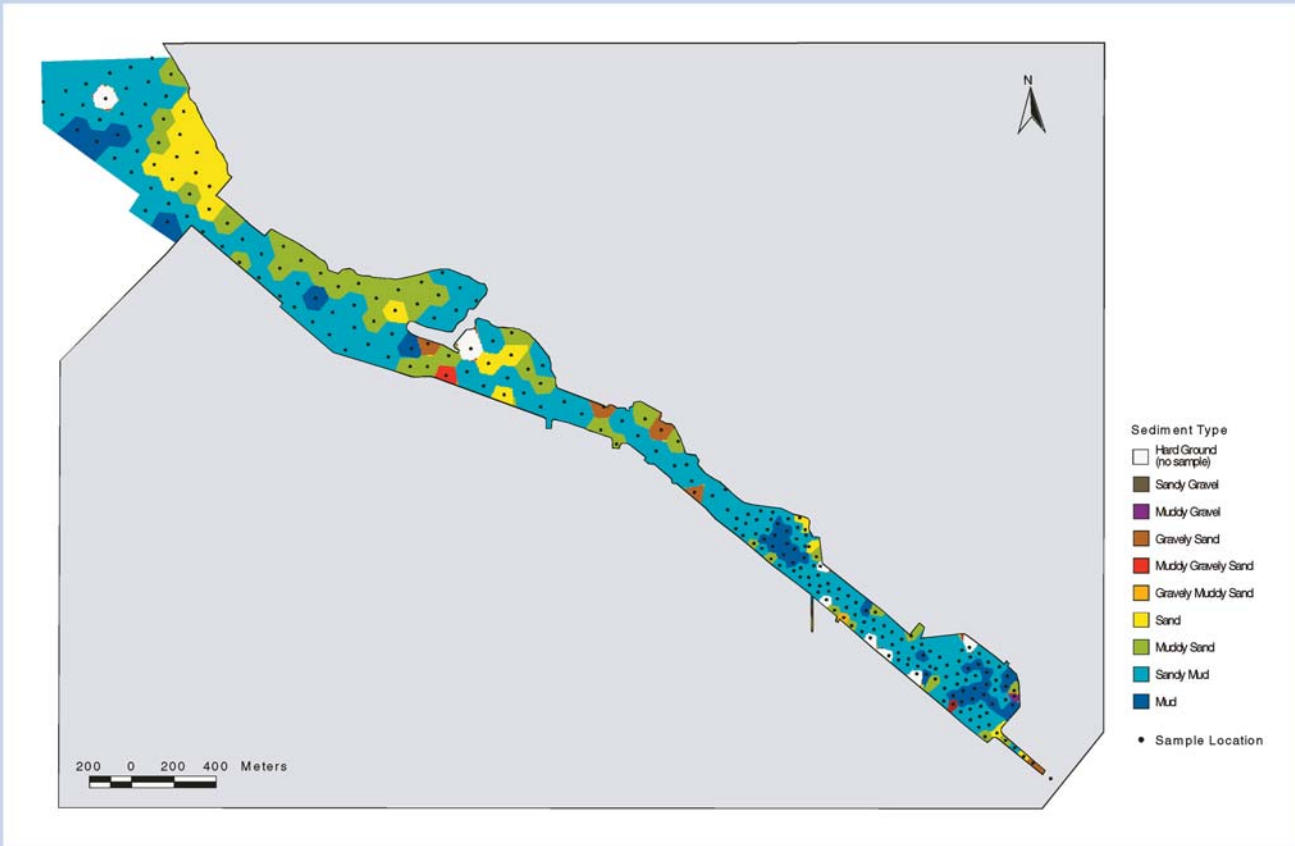

Figure 3. Sediment types found in the Hylebos Waterway (categories are based on 20%, 50%, and 80% cutoffs; e.g., sand is >80% sand-sized material and contains <20% of any other size; muddy sand is >50% sand and >20% mud-sized material; and gravelly muddy sand contains >50% sand and >20% of both gravel- and mud-sized material).

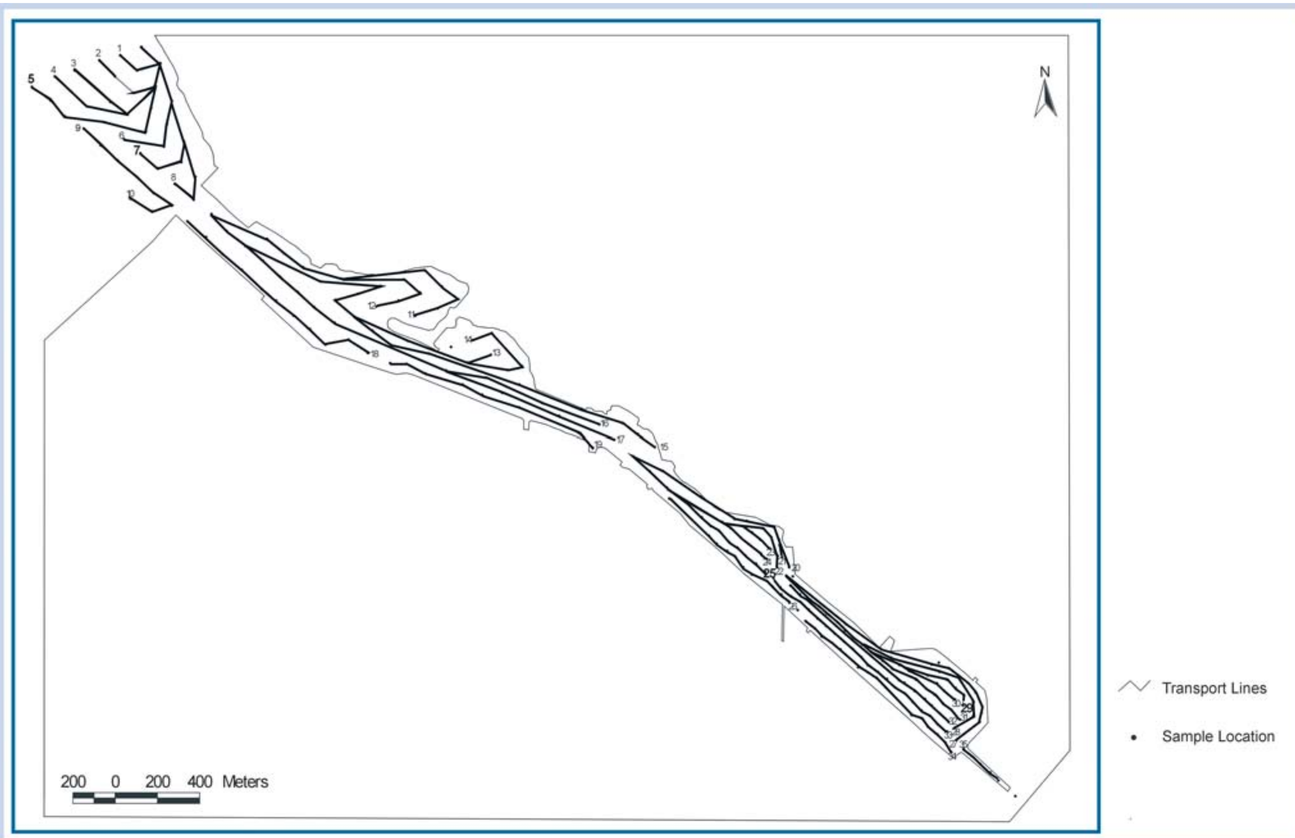

Figure 4. Sample sequences (lines) used in the derivation of the sediment transport pathways. (See Appendix 2 for the line statistics.)

Figure 5. Net sediment transport pathways, dynamic behavior, and corresponding transport environments.

With the exception of some tidal flats on the north side of the outer portion, the banks of the Hylebos Waterway are lined with an extensive industrial complex (Figure 2). Because of past contaminant releases into the area, the Tacoma Tideflats was declared a Superfund Site in the early 1980s.

PATTERNS OF SEDIMENT TRANSPORT

The sediments in the study area range from sandy gravel to mud, with the largest proportion (57%) being sandy mud (Figure 3). The latter sediment type is common throughout the Waterway. Significant patches of mud are found in both the Lower and Upper Turning Basins.

In searching for patterns of sediment transport (the full rationale and technique are described in Appendix 1), it was found that the best and most consistent pathways could be generated with the use of all samples as a single complete data set. Attempts to isolate specific sediment types (e.g., mud or muddy sand) did not yield satisfactory results. It is likely, therefore, that despite the range and mixture of particle sizes present in the Waterway, all samples represent a single facies from which the transport relationships among them can be determined.

Following the calculation of numerous sample sequences, a mutually supportive and coherent pattern of transport that could account for all the sediment grain size distributions required a total of 35 lines or sample sequences (Figures 4 and 5). The trend statistics for each trend line are provided in Appendix 2. These include the Z score statistic, R^2, and the derived interpretation of the dynamic behavior as determined

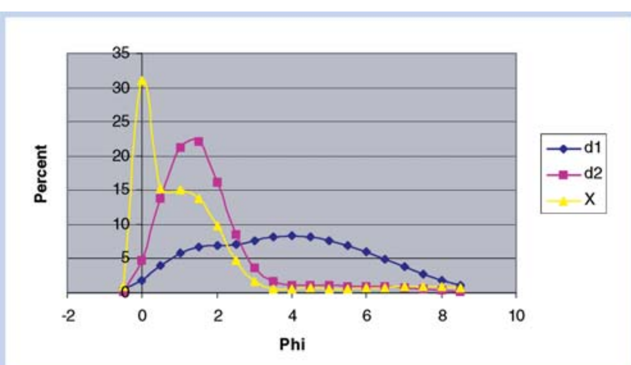

Figure 6. Distributions of d_1, d_2, and X for line 7 (Figure 4) in TE1. The X distribution compared with d_1 and d_2 indicates that Net Erosion is occurring down the line (compare with Figure A6-C).

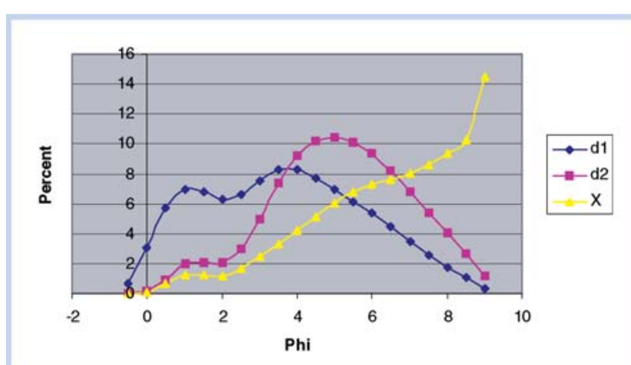

Figure 7. Distributions of d_1, d_2, and X for line 5 (Figure 4) in TE1. The X distribution compared with d_1 and d_2 indicates that Total Deposition (type 1) is occurring down the line (compare with Figure A6-D).

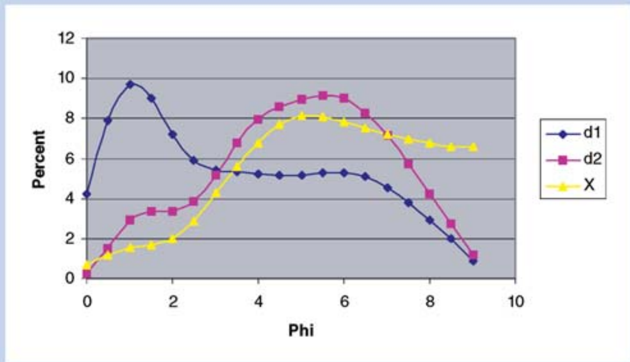

Figure 8. Distributions of d_1, d_2, and X for line 17 (Figure 4) in TE2. The X distribution compared with d_1 and d_2 indicates that Dynamic Equilibrium is occurring down the line (compare with Figure A6-A).

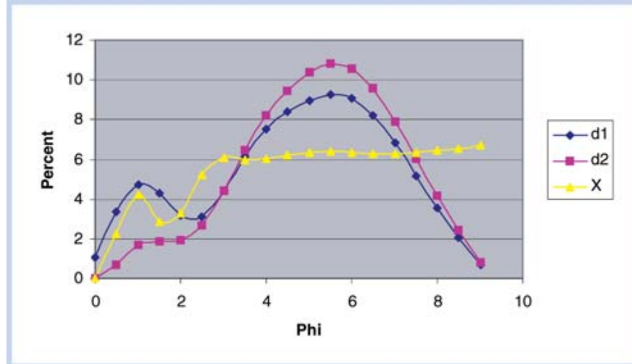

Figure 10. Distributions of d_1, d_2, and X for line 29 (Figure 4) in TE4. The X distribution compared with d_1 and d_2 indicates that Total Deposition (type 2) is occurring down the line (compare with Figure A6-E).

by the $X(s)$ function. For ease of discussion, the pathways are grouped into areas defined as transport environments (TEs; Figure 5). A TE is an area within which transport lines are associated both geographically and by their dominant dynamic behavior. Generally, transport lines cannot be continued from one TE into another (i.e., the trend from one TE into the other will become statistically unacceptable, or ambiguous), so a region in which transport lines naturally end (and begin) defines the intervening boundary.

The following provides a brief description of each TE (Figure 5) together with examples of d_1, d_2, and X distributions.

TE1: Commencement Bay

This TE is confined to Commencement Bay. Evidence that the samples making up this environment could be related to the sediments found immediately inside the Hylebos Waterway was lacking. This environment is composed of relatively few samples and should be accepted with caution. The trends suggest that this part of Commencement Bay is under the influence of a clockwise gyre, with the sediments originating from shoreline glacial deposits on the north side of the Bay. The nearshore trends show Net Erosion (Figure 6), suggesting that foreshore lowering with consequent coastal erosion is likely occurring. In the offshore deeper waters, sediments in the gyre generally fine to muddy sediments, and Total Deposition (type 1) appears to be taking place (Figure 7).

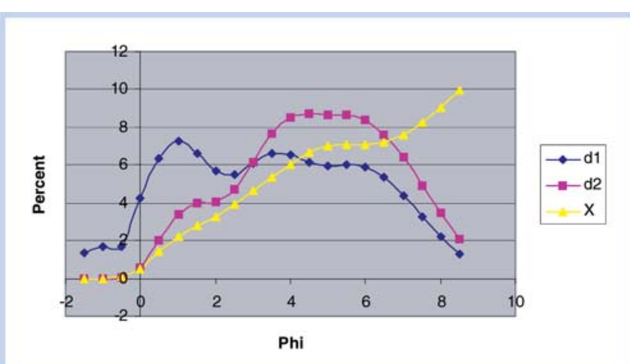

Figure 9. Distributions of d_1, d_2, and X for line 25 (Figure 4) in TE3. The X distribution compared with d_1 and d_2 indicates that Total Deposition (type 1) is occurring down the line (compare with Figure A6-D).

TE2: Outer Waterway

This environment originates at the entrance to the Waterway and extends to slightly more than one-half its length. Most of the trends are in Dynamic Equilibrium (Figure 8), a finding that is relatively rare in muddy sediments, which because of their cohesive properties, tend to form deposits of Total Deposition. The finding of Dynamic Equilibrium suggests that processes capable of resuspending the muddy sediments enable transport to continue up the Waterway. A probable process that would result in resuspension is propeller wash.

TE3: Middle Waterway

Originating in a slightly narrower part of the Waterway, these lines continue with transport up the channel and terminate in the mud associated with the Lower Turning Basin. Nearly all the lines are defined by Total Deposition (type 1) dynamic behavior (Figure 9). Unlike the outer Waterway (TE2), these sediments are evidently less susceptible to resuspension, probably because 1) the sediment has become finer and is therefore more cohesive than the sediments in the outer Waterway, 2) shipping activity might decrease with increasing distance from the mouth of the Waterway, and 3) currents are known to decrease with distance up the Waterway (Norton and Barnard 1992).

TE4: Inner Waterway

Commencing in the narrows up-channel from the Lower Turning Basin, landward transport continues into the Upper Turning Basin. Nearly all the pathways produced X distributions indicative of Total Deposition (type 2; Figure 10). Such behavior suggests that much of the coarser grain sizes in the channel have already been deposited, undoubtedly in the Lower Turning Basin, and the remaining sizes left to continue up-channel are extremely fine (i.e., all remaining sizes have an equal probability of being deposited).

TE5: Hylebos Creek

Consisting of a single line of samples taken in Hylebos Creek, this environment indicates coarse sediment in Dynamic Equilibrium flowing toward the Upper Turning Basin. The influence of the creek does not appear to be particularly significant with respect to the marine sedimentation that characterizes the Waterway.

Table 1. Summary of sediment and contaminant dynamic behaviors on the basis of sediment trend analysis (STA) and the *X* distribution

Sediment dynamic behavior (stability)	The shape of $X(s)$ relative to $d_1(s)$ and $d_2(s)$ (see Figure A6)	Contaminant dynamic behavior
Net Erosion	The mode of $X(s)$ is coarser than the $d_1(s)$ and $d_2(s)$ modes. More grains are eroded than deposited, and sediment coarsens along the transport path.	Contaminant levels decrease rapidly down the transport path and are dispersed to areas of deposition.
Net Accretion	The mode of $X(s)$ is finer than the modes of $d_1(s)$ and $d_2(s)$. More grains are deposited than eroded, and accretion occurs down the transport path.	Contaminant levels increase down the transport pathway.
Dynamic Equilibrium	The modes of all 3 distributions are the same. The probability of finding a particular grain in the deposit is equal to the probability of its transport and redeposition (i.e., replacement is grain-by-grain along the transport path). The bed is neither accreting nor eroding and is, therefore, in Dynamic Equilibrium.	Contaminated sediments will move down the transport pathway while remaining as a coherently defined hotspot.
Total Deposition (type 1)	The $X(s)$ distribution increases monotonically over the complete $d_1(s)$ and $d_2(s)$ distributions. Sediment fines in the direction of transport; however, the bed is no longer mobile. Once deposited, no further transport occurs.	Contaminated sediments form localized hotspots that undergo no further transport.
Total Deposition (type 2)	$X(s)$ is horizontal. This type of X distribution is found only in extremely fine sediments when the mean grain size is very fine silt or clay, Such sediments are usually found far from their source (compared with Total Deposition (type 1) sediments. Deposition is no longer related strictly to size sorting. All sizes have an equal probability of being deposited down the transport path.	Contaminated particles have an equal probability of being deposited anywhere in this type of environment. Hot spots do not form; rather, contaminant concentrations will be relatively equal throughout the depositional area.

PROCESS IMPLICATIONS

Despite considerable efforts to find reversals or a more complex pattern of sediment transport in the Waterway, the derived patterns of net sediment transport for the Hylebos show movement entirely in an up-channel direction (from the mouth toward the head of the Waterway). Furthermore, the dynamic behavior of the transport regime changes in a regular way from Dynamic Equilibrium in TE2 (outer Waterway), followed by Total Deposition (type 1) in the sediments associated with the Lower Turning Basin (middle Waterway TE3), and ending with extremely fine sediments in Total Deposition (type 2) in TE4 (inner Waterway). This progressive change in dynamic behavior suggests that sediments become increasingly finer (and increasingly cohesive) toward the upper end of the Waterway together with a decrease in current velocities. The latter is reported in Norton and Barnard (1992), in which velocities at the mouth were up to 10 cm/s compared with those at the head, where they were generally less than 2 cm/s. Floyd and Snider Inc. (1998) described the presence of underlying dense water masses that move regularly into the Hylebos Waterway as a result of upwelling from Commencement Bay. A similar stratification was observed by Loehr et al. (1981), in which flood tidal currents prevailed near the bottom and surface, with a midlayer favoring the ebb. Both current velocities and the stratification can be disturbed by vessel activities inducing mixing and possible scour (Floyd and Snider Inc. 1998).

It is quite likely that the observed changes in dynamic behavior toward the head is also influenced by a decreasing number of vessel passages in the channel (i.e., given that

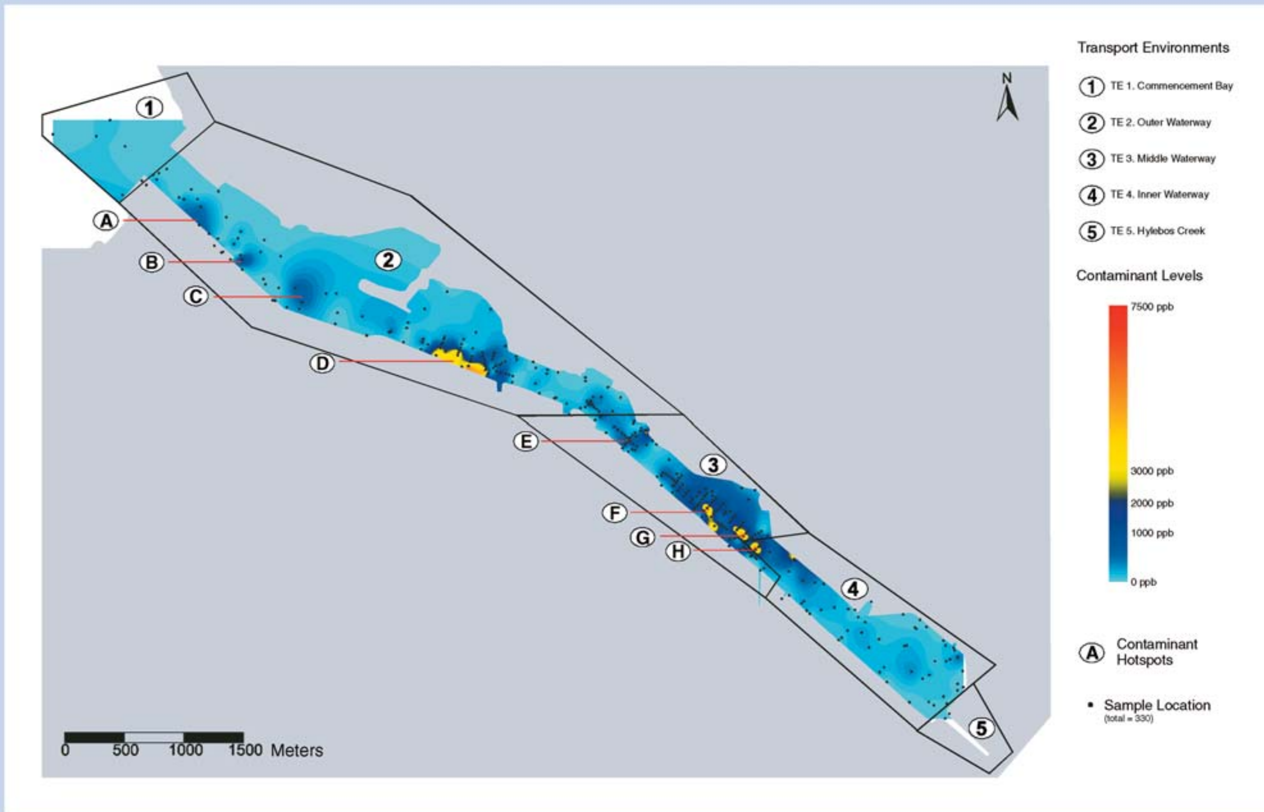

Figure 11. The distribution of total pesticides and polychlorinated biphenyls (PCBs) contained in the sediments of the Hylebos Waterway.

docks line most of the channel, more vessels can be expected to pass back and forth in TE2 (outer Waterway) creating conditions favorable for resuspension and Dynamic Equilibrium than in TEs 3 and 4, in which Total Deposition prevails). Such resuspension events in TE3 might provide an opportunity for further transport from TE3 into TE4, after which no further area is left to which sediment can be transported regardless of vessel traffic.

It is interesting that sediments in TE1 (Commencement Bay) could not be related by transport to sediments in the Waterway. In other words, there must be a significant source present in the Waterway that is not as important in the Commencement Bay environment. Two possible explanations are probably both operating. The 1st is that suspended sediment associated with the Puyallup River plume, although negligible compared with the source of sediments that are provided by a lowering foreshore along the north side of Commencement Bay, becomes a significant sediment input once inside the Waterway. Second, industrial activity and the presence of various outfalls are likely contributing a miscellany of sediment types unique to the Waterway (note that many of the isolated patches of coarse and mixed sediments are found along its banks; Figure 3).

RELATIONSHIP BETWEEN STA AND CONTAMINANT LEVELS

The relationship between contaminant levels contained in sediments with the texture and stability of the sediments themselves is now known to be highly complex and is the subject of considerable research (e.g., Apitz et al. 2004). Site-specific conditions can result, for example, in a uniform distribution of contaminants throughout the particle size range of their associated sediments. In other instances, the distribution of contaminants could show bimodality, with modes associated with both fine and coarse sediment fractions. It has, however, long been recognized that many contaminants tend to associate preferentially with the finer sediment fractions as opposed to the coarser sizes and that pollutants tend to follow the same transport pathways of sedimentary material, tending to be transported to depositional sinks regardless of the exact source of contamination (Young et al. 1985).

In the context of STA, and on the basis of the assumption that contaminants will preferentially follow net sediment transport pathways, McLaren and Little (1987) predicted the accumulation and dispersal of hydrocarbons and heavy metals throughout a small estuary in southwest Wales. It was found that the relationship between the predicted concentrations in different portions of the estuary with actual measured concentrations produced a highly significant correlation (Spearman's rank correlation coefficient of 0.98, where 1.0 indicates complete agreement between the expected order of contaminant concentrations with the observed order of concentrations). Since this finding, the empirically derived relationships between contaminant levels contained in sediments and the results of STA have both improved and been supported in a number of studies (e.g., McLaren et al. 1993; Pascoe et al. 2002). These relationships, based on all the assumptions made in carrying out STA (see Appendix 1), are summarized in Table 1.

IMPLICATIONS FOR CONTAMINANTS

On the basis of the correlation between sediment stability and contaminant behavior (Table 1), it is instructive to consider the probable behavior of contaminated particles in the Waterway in the absence of local contaminant sources. Assuming that a source of contaminated particles enters the Waterway at its mouth, the 1st environment encountered (TE2, outer Waterway) is predominantly in Dynamic Equilibrium. Contaminated particles deposited in this environment will tend to have an equal probability of continuing up-channel transport as on a conveyor belt. Hot spots might develop at random but will tend to move toward the Lower Turning Basin given sufficient time.

The conveyor belt form of transport ends at the start of TE3 (middle Waterway), an environment dominated by Total Deposition (type 1). Here, contaminated particles will come out of transport to form 1 or more hotspots that are unlikely to be easily dispersed. Thus, the Lower Turning Basin is expected to be an important contaminant sink.

Finally, TE4 (inner Waterway) is dominated by Total Deposition (type 2), an environment in which the remaining particles in transport are sufficiently fine that they escaped deposition in the Lower Turning Basin and now have an equal probability of deposition anywhere in the Upper Turning Basin. Specific hotspots would be unlikely; however, a ubiquitous contaminant level throughout the environment would more probably be observed. It is emphasized that throughout all 3 of the Hylebos TEs, it would be very unlikely for a contaminated particle contained in the sediments to have the opportunity to move in the reverse direction toward the mouth.

In reality, the high level of industry surrounding the Waterway has resulted in numerous contaminant sources. Like sediment, the greater the amount of contaminant entering the environment, the greater the probability of its deposition in the sediment regardless of the dynamic behavior. For example, a significant contaminant source in TE2 (outer Waterway), in which the sediments are predominantly in Dynamic Equilibrium, could well form local hotspots by simply overwhelming the sedimentary environment. Although the hotspot might be dispersed in the up-channel direction, without an effective source control program, the original hotspot will be continually replenished.

To relate the findings of the STA with known contaminant levels, a contaminant database was made available to GeoSea (Striplin and Associates, Olympia, WA, USA). Because of the large size of the database and the extensive number of organic and heavy metals available, it was necessary to make various practical decisions. Some data collected during particular surveys were not described well enough in the provided documentation to be used with confidence. The database was ultimately edited to include only surface samples.

Numerous maps of various contaminants were constructed with the aid of Surfer®, a contouring and 3-dimensional surface mapping software package made by Golden Software (Golden, CO, USA). It was found that separate maps of the organic compounds generally produced similar patterns, as did separate maps of the trace metal data. For this paper, a map of total pesticides and polychlorinated biphenyls (PCBs) has been chosen to provide an appropriate illustration of the findings (Figure 11).

The relationship between the defined TEs (Figure 5) and contaminant levels (Figure 11) appears to be consistent with the expected findings as described in Table 1. In TE2 (outer Waterway), several isolated hotspots exist (shown as A, B, C, and D in Figure 11). Not all the hotspots are necessarily related to an immediate shoreline source (e.g., hotspots B and C), and these might well be interpreted as random locations in an environment of Dynamic Equilibrium, in which the contaminants are contained within a sediment conveyor belt moving toward the head of the Waterway. Hotspots E, F, G, and H are nearly all out in midchannel (i.e., no immediate shoreline source) and appear relatively isolated, as expected in an environment of Total Deposition (type1). Finally, TE4 (inner Waterway) shows a more or less equal spread of values throughout, which is also expected in an environment of Total Deposition (type 2).

RESOLUTION OF LIABILITY ALLOCATION ISSUES

Sediment trend analysis assumes that the probability of sediment movement is based on particle size and that the relationship between transport pathways and contaminant levels is dependent on contaminants preferentially associating with the finer rather than coarser size fractions of the available sediment. In situations in which such assumptions might not be valid, any correlation between the pathways and contaminants would be unlikely. When such a correlation does exist, however, the findings, together with other available evidence, could help to resolve liability issues. For the Hylebos Waterway, the results of the STA were applied as part of an analysis of the potential legal liability of parties who might have been sources of the contamination found in the sediments. The potential legal liability included liability to the USEPA for the cleanup of the contaminated sediments, liability to Natural Resource Trustee agencies for natural resource damages (NRDs) caused by the contaminated sediments, and liability allocation among the potentially responsible parties (PRPs) for these costs.

The most striking finding of the STA from a liability standpoint was the net sediment transport from the mouth of the Waterway toward the head. This evidence was used in liability allocation negotiations to demonstrate that PRPs located at the head of the Waterway might not be responsible for contaminated sediments at the mouth of the Waterway. Similarly, PRPs located sediment downstream (i.e., toward the head) of the highly contaminated Lower Turning Basin are unlikely to be responsible for the contaminated sediments there.

The information on the defined TEs, particularly the areas of dynamic equilibrium, was used in allocation negotiations to demonstrate that the sources of several of the isolated hotspots up the Waterway were actually from PRPs located farther down near the mouth of the Waterway, and not from the immediately adjacent properties. From an allocation perspective, the major documented sources of contamination at the mouth of the Waterway should be expected to bear a large share of the total cleanup and NRD liability for the entire Hylebos, because of the dynamic migration of sediment contamination from these sources toward the Head.

The STA information was used to supplement analyses of the patterns of sediment concentration gradients that had previously been used to identify likely source properties. In many cases, the STA analysis helped explain apparent anomalies in the sediment concentration gradients. For instance, the STA explained how hot spots of PCBs could be located near a property in which PCBs had never been released to the environment. If sediment gradient pattern analysis alone were used to allocate liability among PRPs, the PRPs located near these hot spots would receive a disproportionate share of liability.

The STA results were also used during negotiations to rebut an assumption by the NRD Trustee agencies that contaminated sediments from a particular source would be as likely to migrate down as up the Waterway. The STA showed that this sediment distribution assumption was invalid. Such a change in assumptions had a dramatic effect on allocation calculations.

Other information useful to liability analysis included the conclusion that sediments outside of the Waterway in Commencement Bay are separate from the Waterway. This information shows that PRPs responsible for contaminated sediments within the Waterway are unlikely to be sources of contamination found in sediments outside of the Waterway, even in the immediate vicinity of the mouth of the Hylebos.

SUMMARY AND CONCLUSIONS

1. An STA was performed with the use of 242 sediment samples taken from the Hylebos Waterway. Most of the samples (57%) are sandy mud, although sediments generally fine in the channel from its mouth to its head. Significant patches of mud are located in each of the 2 turning basins. All samples were used as a single facies to derive the sediment trends.
2. Thirty-five sample sequences (lines) were selected to describe the best possible transport pathways, and these divided into 5 distinct TEs extending from the mouth to the head of the Waterway.
3. The STA revealed that sediments immediately outside the Waterway in Commencement Bay are separate from those inside the Waterway. This is explained by the dominance of a shoreline source along the north shore of Commencement Bay, most of which does not enter the Waterway. The latter contains sediments from a variety of shoreline sources (often a result of industrial activities) as well as fine sediment input from the Puyallup River plume. It is the combination of these 2 sources that causes the Waterway sediments to be uniquely different from those in Commencement Bay.
4. The trends inside the Waterway all showed net sediment movement toward its head. The dynamic behavior changed progressively from Dynamic Equilibrium in the outer Waterway (TE2), to Total Deposition (type 1) behavior in the middle Waterway (TE3), to Total Deposition (type 2) in the inner Waterway (TE4). These findings correspond well with known processes in which tidal flood currents dominate and are stronger nearer the mouth than the head of the Waterway.
5. Vessel traffic is likely helpful in resuspending sediment in TE2, resulting in Dynamic Equilibrium as well as enabling some further movement from TE3 into TE4. If sediments were disturbed by propeller wash in TE4, they would likely remain in that environment.
6. The sediment trends suggest that, in the event of a contaminant entering the Waterway and becoming associated with the sediments, its movement toward the mouth would be extremely unlikely compared with its movement toward the head.
7. On the basis of the assumptions that contaminants will follow the transport patterns of natural sediments and associate preferentially with the finer particle size fractions, existing contaminant data appear to correlate well with the findings of the STA. The dynamic behavior of TE2 suggests that contaminant hotspots would be random and, in the long term, ephemeral as they move in a conveyor belt fashion toward the head of the Waterway. In TE3, hotspots are likely to form and remain stationary, with little or no further movement, whereas in TE4, hotspots would be less likely. Instead contaminant levels would be relatively evenly distributed over the entire area of the TE.
8. The relationships described in point 7 are somewhat obscured by the presence of significant shoreline sources of contaminants evidently entering the Waterway. At such places, the abundance of the source can, at least temporarily, overwhelm the effects of the existing dynamic behavior of the receiving sediments. Nevertheless, maps of contaminant levels in the sediment correlate well with the TEs defined by the STA.
9. Sediment trend analysis demonstrated that PRPs located toward the head of the Waterway should not be allocated cleanup or NRD costs for contaminated sediments located toward the mouth of the Waterway. Similarly, PRPs with documented sources near the mouth of the Waterway should be allocated a large share of total cleanup and NRD costs for the entire Waterway because contaminated sediments migrate up the Waterway and deposit at the head of the Waterway. The STA also helped explain apparent anomalies in the patterns of sediment concentration gradients.

Acknowledgment—The authors thank S. Heise of the Technische Universität Hamburg–Harburg, Germany, and 1 anonymous reviewer for particularly constructive comments on the manuscript. This project was funded by one of the private industial stakeholders of the Hylebos Waterway.

REFERENCES

Apitz SE, Ayers V, Kirtay VJ. 2004. Use of data on contaminant/sediment interactions to streamline sediment assessment and management. San Diego (CA): US Navy SPAWAR Systems Center. Tech report 1918. August 2004. 122 p.

Apitz SE, Davis JW, Finkelstein K, Hohreiter DW, Hoke R, Jensen RH, Jersak J, Kirtay VJ, Mack EE, Magar VS, Moore D, Reible D, Stahl RG. 2005. Assessing and managing contaminated sediments: Part I, developing an effective investigation and risk evaluation strategy. *Integr Environ Assess Manag* 1:2–8.

Chang YH, Scrimshaw MD, Lester JN. 2001. A revised grain-size trend analysis program to define net sediment transport pathways. *Comput Geosci* 27:109–114.

Floyd and Snider Inc. 1998. Circulation, water properties, and ship-induced scour. Seattle (WA): Hylebos Waterway wood debris program, events 1A and 1B data report, agency draft, 7/8/98.

Gao S. 1996. A Fortran program for grain-size trend analysis to define net sediment transport pathways. *Comput Geosci* 22:449–452.

Gao S, Collins M. 1991. A critique of the "McLaren method" for defining sediment transport paths. *J Sediment Petrol* 61:143–146.

Gao S, Collins M. 1992. Net sediment transport patterns inferred from grain-size trends, based upon definition of "transport vectors." *Sediment Geol* 80:47–60.

Hughes SA. 2005. Use of sediment trend analysis (STA®) for coastal projects. Vicksburg (MS): US Army Corps of Engineers ERDC/CHL CHETN-VI-40. 17 p.

Le Roux JP. 1994. An alternative approach to the identification of net sediment transport paths based on grain-size trends. *Sed Geol* 94:97–107.

Le Roux JP, O'Brian RD, Rios F, Cisternas M. 2002. Analysis of sediment transport paths using grain-size parameters. *Comput Geosci* 28:717–721.

Loehr LC, Collias EE, Sullivan RH, Haury D. 1981. Commencement Bay studies technical report, Vol. VI, physical oceanography. Seattle (WA): Prepared by Dames & Moore for the US Army Corps of Engineers, Seattle District.

McLaren P, Bowles D. 1985. The effects of sediment transport on grain-size distributions. *J Sediment Petrol* 55:457–470.

McLaren P, Cretney WJ, Powys RIL. 1993. Sediment pathways in a British Columbia fjord and their relationship with particle-associated contaminants. *J Coast Res* 9:1026–1043.

McLaren P, Little DI. 1987. The effects of sediment transport on contaminant dispersal: An example from Milford Haven. *Mar Pollut Bull* 14:586–594.

Norton D, Barnard R. 1992. Spatial and temporal trends in contaminant levels in settling particulate matter: Hylebos Waterway (Commencement Bay), July 1990 to November 1991. Olympia (WA): Washington State Department of Ecology, Environmental Investigations and Laboratory Services Program, Toxic Compliance and Ground Water Monitoring Section. Water Body WA-10–0020 (Segment 05–10–01). 43 p + Appendices.

Pascoe GA, McLaren P, Soldate M. 2002. Impact of offsite sediment transport and toxicity on remediation of a contaminated estuarine bay. *Mar Pollut Bull* 44:1184–1193.

Rios F, Ulloa R, Cerrea ICS. 2003. Determination of net sediment transport patterns in Lirquen Harbor, Chile through grain-size analysis: A test of methods. *Pesquisas em Geociencias* 30:65–81.

[USEPA] US Environmental Protection Agency. 2002. Principles for managing contaminated sediment risks at hazardous waste sites. Washington (DC): Office of Solid Waste and Emergency Response (OSWER). OSWER directive 9285.6–08.

Young RA, Swift DJP, Clarke TL, Harvey GR, Betzer PR. 1985. Dispersal pathways for particle associated pollutants. *Science* 229:431–435.

Integrated Environmental Assessment and Management — Volume 2, Number 3 — pp. e8–e19

Sediment Trend Analysis of the Hylebos Waterway: Implications for Liability Allocations

Patrick McLaren† and R Paul Beveridge‡*

†GeoSea® Consulting (Canada), 7236 Peden Lane, Brentwood Bay, British Columbia V8M 1C5
‡Heller Ehrman LLP, 701 Fifth Avenue, Suite 6100, Seattle, Washington 98104-7098, USA

Appendix 1

SEDIMENT TREND ANALYSIS

The following provides a review, discussion, and description of how sediment transport pathways are obtained. It excludes the details of the mathematical proof, demonstrating the changes in grain size distributions that occur with transport as contained in McLaren and Bowles (1985).

Sediment trend analysis (STA) requires for its data the grain size distributions of sediments collected on regular grid spacing over the aquatic site of interest. The sampled sediments are described in statistical terms (by the moment measures of mean, sorting, and skewness), and the basic underlying assumption is that processes causing sediment transport will affect the statistics of the sediments in a predictable way. For this purpose, a grain size distribution defines for any size class the probability of the sediment being found in that size class. Size classes are defined in terms of the well-known ϕ (phi) unit, where d is the effective diameter (diameter of the sphere with equivalent volume) of the grain in millimeters.

$$d(\mathrm{mm}) = 2^{-\phi} \quad \text{or} \quad \log_2 d(\mathrm{mm}) = -\phi \tag{1}$$

Given that the grain size distribution $g(s)$, where s is the grain size in phi units, is a probability distribution, then

$$\int_{-\infty}^{\infty} g(s)ds = 1 \tag{2}$$

In practice, grain size distributions do not extend over the full range of s and are not continuous functions of s. Instead, discretized versions of $g(s)$ with estimates of $g(s)$ in finite-sized bins of 0.5ϕ widths are used. Selection of the bin width is largely empirically derived. An increase in width can result in losing information contained in the distribution, whereas a decrease in width can produce an increasingly noisy distribution (a discussion of this dilemma is found in Bowles and McLaren [1985]).

Three parameters related to the first 3 central moments of the grain size distribution are of fundamental importance in STA. They are defined here, both for a continuous $g(s)$ and for its discretized approximation with N size classes. The 1st parameter is the mean grain size (m), defined as

$$\mu = \int_{-\infty}^{\infty} s g(s)\, ds \approx \sum_{i=1}^{N} s_i g(s_i) \tag{3}$$

The 2nd parameter is sorting (s), which is equivalent to the variance of the distribution, defined as

$$\sigma^2 = \int_{-\infty}^{\infty} (s-\mu)^2 g(s)\, ds \approx \sum_{i=1}^{N} (s_i-\mu)^2 g(s_i) \tag{4}$$

Finally, the coefficient of skewness (k) is defined as

$$\kappa = \frac{1}{\sigma^3}\int_{-\infty}^{\infty} (s-\mu)^3 g(s)\, ds \approx \frac{1}{\sigma^3}\sum_{i=1}^{N} (s_i-\mu)^3 g(s_i) \tag{5}$$

Case A: Development of a lag deposit

Consider a sedimentary deposit that has a grain size distribution $g(s)$ (Figure A1). If eroded, the sediment that goes into transport has a new distribution, $r(s)$, that is derived from $g(s)$ according to the function $t(s)$, so that

$$r(s_i) = kg(s_i)t(s_i) \quad \text{or} \quad t(s_i) = \frac{r(s_i)}{kg(s_i)} \tag{6}$$

where $g(s_i)$ and $r(s_i)$ define the proportion of the sediment in the ith grain size class interval for each of the sediment distributions and k is a scaling factor that normalizes $r(s)$ to get Equation 7. (The scaling factor k is actually more complex than a simple normalizing function, and its derivation and meaning is the subject of further research. It appears to take into account the masses of sediment in the source and in transport and might be related to the relative strength of the transporting process.)

$$\sum_{i=1}^{N} r(s_i) = 1 \quad \text{thus} \quad k = \frac{1}{\sum_{i=1}^{N} g(s_i)t(s_i)} \tag{7}$$

With the removal of $r(s)$ from $g(s)$, the remaining sediment (a lag) has a new distribution denoted by $l(s)$ (Figure A1) where

$$l(s_i) = kg(s_i)[1-t(s_i)] \quad \text{or} \quad t'(s_i) = \frac{l(s_i)}{kg(s_i)} \quad \text{where} \quad t'(s_i) = 1 - t(s_i) \tag{8}$$

The function $t(s)$ is defined as a sediment transfer function and is described in exactly the same manner as a grain size probability function except that it is not normalized. It can be thought of as a function that incorporates all sedimentary and dynamic processes that result in initial movement and transport of particular grain sizes.

Data from flume experiments show that distributions of transfer functions change from having a high negative skewness to being nearly symmetrical (although still negatively skewed) as the energy of the eroding/transporting process increases. These 2 extremes in the shape of $t(s)$ are termed low-energy and high-energy transfer functions, respectively (Figure A2). The shape of $t(s)$ is also dependent not only on changing energy levels of the process involved in erosion and transport, but also on the initial distribution of the original bed material, $g(s)$ (Figure A1). The coarser $g(s)$ is,

* To whom correspondence may be addressed patrick@geosea.ca

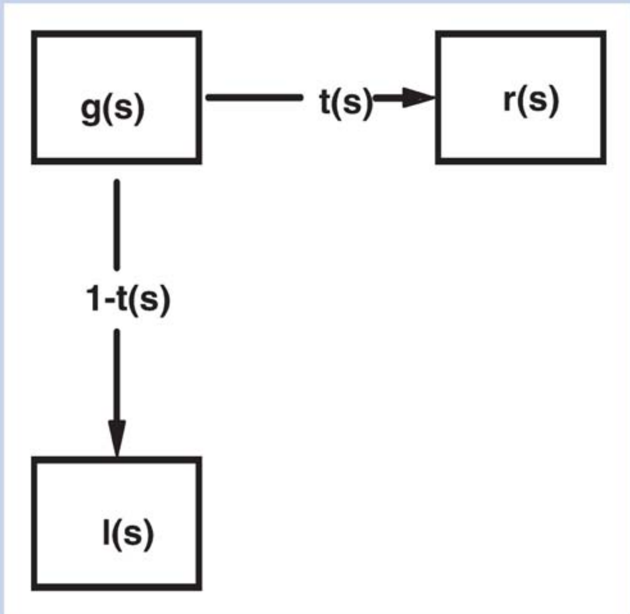

Figure A1. Sediment transport model to develop a lag deposit (see the text for a definition of terms).

the less likely it is to be acted on by a high-energy transfer function. Conversely, the finer $g(s)$ is, the easier it becomes for a high-energy transfer function to operate on it. In other words, the same process can be represented by a high-energy transfer function when acting on fine sediments and by a low-energy transfer function when acting on coarse sediments. The terms high and low energy are, therefore, relative to the distribution of $g(s)$ rather than to the actual process responsible for erosion and transport.

That $t(s)$ appears to be mainly a negatively skewed function results in $r(s)$, the sediment in transport, always becoming finer and more negatively skewed than $g(s)$. The function $1 - t(s)$ (Figure A1) is, therefore, positively skewed, with the result that $l(s)$, the lag remaining after $r(s)$ has been removed, will always be coarser and more positively skewed than the original source sediment. McLaren and Bowles (1985) provide the mathematical proof for these statements.

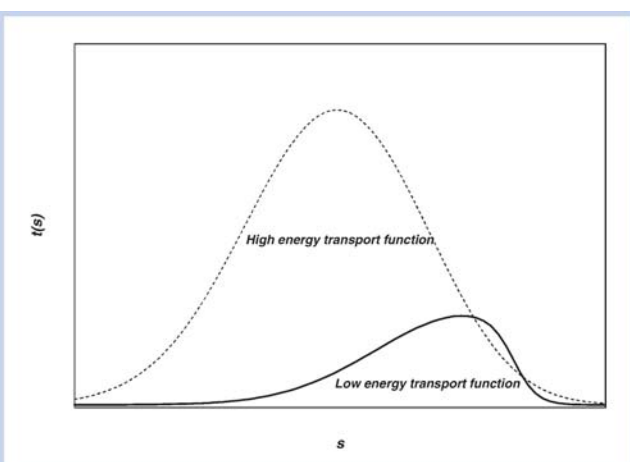

Figure A2. Diagram showing the extremes in the shape of transfer functions $t(s)$.

If $t(s)$ is applied to $g(s)$ many times (i.e., n times, where n is large), then the variance of both $g(s)$ and $l(s)$ will approach zero (i.e., sorting will become better). Depending on the initial distribution of $g(s)$, it is mathematically possible for variance to become greater before eventually decreasing. In reality, an increase in variance in the direction of transport is rarely observed.

Given 2 sediments whose distributions are, $d_1(s)$ and $d_2(s)$, and $d_2(s)$ is coarser, better sorted, and more positively skewed than $d_1(s)$, it might be possible to infer that $d_2(s)$ is a lag of $d_1(s)$ and that the 2 distributions were originally the same (Table A1, case A).

Case B: Sediments become finer in the direction of transport

Consider a sequence of deposits $d_1(s)$, $d_2(s)$, $d_3(s)$, ... $d_n(s)$ that follows the direction of net sediment transport (Figure A3). Each deposit is derived from its corresponding sediment in transport according to the 3-box model shown in Figure A1. Each $d_n(s)$ can be considered a lag of each $r_n(s)$. Thus, $d_n(s)$ will be coarser, better sorted, and more positively skewed than $r_n(s)$. Similarly, each $r_n(s)$ is acted on by its corresponding $t_n(s)$, with the result that the sediment in transport becomes progressively finer, better sorted, and more negatively skewed. Any 2 sequential deposits (e.g., $d_1[s]$ and $d_2[s]$) can be related to each other by a function $X(s)$ (Eqn. 9).

$$d_2(s) = kd_1(s)X(s)$$

$$\text{or } X(s) = \frac{d_2(s)}{kd_1(s)} \tag{9}$$

$$\text{where } k = \frac{1}{\sum_{i=1}^{N} d_1(s_i)X(s_i)}$$

As illustrated in Figure A3, $d_2(s)$ can also be related to $d_1(s)$ by

$$d_2(s) = \frac{kd_1(s)t_1(s)[1 - t_2(s)]}{1 - t_1(s)}$$

$$= kd_1(s)X(s) \tag{10a}$$

$$\text{where } X(s) = \frac{t_1(s)[1 - t_2(s)]}{1 - t_1(s)} \tag{10b}$$

The function $X(s)$ combines the effects of 2 transfer functions, $t_1(s)$ and $t_2(s)$ (Eqn. 10b). It could also be considered a transfer function in that it provides the statistical relationship between the 2 deposits and it incorporates all of the processes responsible for sediment erosion, transport, and deposition. The distribution of deposit $d_2(s)$ will, therefore, change relative to $d_1(s)$ according to the shape of $X(s)$, which in turn is derived from the combination of $t_1(s)$ and $t_2(s)$ as expressed in Equation 10b. It is important to note that $X(s)$ can be derived from the distributions of the deposits $d_1(s)$ and $d_2(s)$ (Eqn. 10a), and it provides the relative probability of any particular sized grain being eroded from d_1, transported, and deposited at d_2.

With the use of empirically derived $t(s)$ functions, it can be shown that when the energy level of the transporting process decreases in the direction of transport (i.e., $t_2[s_i] < t_1[s_i]$) and both are low-energy functions, then $X(s)$ is always a negatively skewed distribution (Figure A4). This will result

Table A1. Summary of the interpretations with respect to sediment transport trends when one deposit is compared with another

Case	Relative change in grain size distribution between deposit d_2 and deposit d_1	Interpretation
A	Coarser Better sorted More positively skewed	d_2 is a lag of d_1. No direction of transport can be determined.
B	Finer Better sorted More negatively skewed	1) The direction of transport can be from d_1 to d_2. 2) The energy regime is decreasing in the direction of transport. 3) t_1 and t_2 are low-energy transfer functions.
C	Coarser Better sorted More positively skewed	1) The direction of transport can be from d_1 to d_2. 2) The energy regime is decreasing in the direction of transport. 3) t_1 is a high-energy transfer function, and t_2 is a high- or low-energy transfer function.

in $d_2(s)$ becoming finer, better sorted, and more negatively skewed than $d_1(s)$. Therefore, given 2 sediments (d_1 and d_2), where $d_2(s)$ is finer, better sorted, and more negatively skewed than $d_1(s)$, it might be possible to infer that the direction of sediment transport is from d_1 to d_2 (Table A1).

Case C: Sediments become coarser in the direction of transport

In the event that $t_1(s)$ is a high-energy function and $t_2(s_i) < t_1(s_i)$ (i.e., energy is decreasing in the direction of transport), the result of Equation 10b will produce a positively skewed $X(s)$ distribution (Figure A4). Therefore, $d_2(s)$ will become coarser, better sorted, and more positively skewed than $d_1(s)$ in the direction of transport. When these changes occur between 2 deposits, it might be possible to infer that the direction of transport is from d_1 to d_2 (Table A1).

Sediment coarsening along a transport path will be limited by the ability of $t_1(s)$ to remain a high-energy function. As the deposits become coarser, it will be less and less likely that the transport processes will maintain high-energy characteristics. With coarsening, the transfer function will eventually revert to its low-energy shape (Figure A2), with the result that the sediment must become finer again.

Cases A and C produce identical grain size changes between d_1 and d_2 (Table A1). Generally, however, the geological interpretation of the environments being sampled will differentiate between the 2 cases.

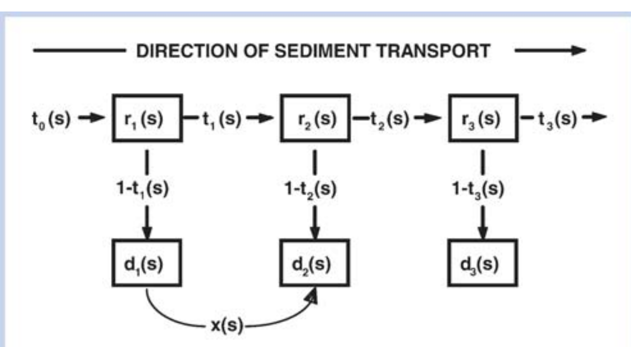

Figure A3. Sediment transport model relating deposits in the direction of transport.

METHOD TO DETERMINE TRANSPORT DIRECTION FROM GRAIN SIZE DISTRIBUTIONS

The above model indicates that grain size distributions of sedimentary deposits will change in the direction of net sediment transport according to either case B or case C (Table A1 and Figure A5). Thus, if any 2 samples (d_1 and d_2) are compared sequentially (i.e., at 2 locations within a sedimentary facies) and their distributions are found to change in the described manner, the direction of net sediment transport can be inferred.

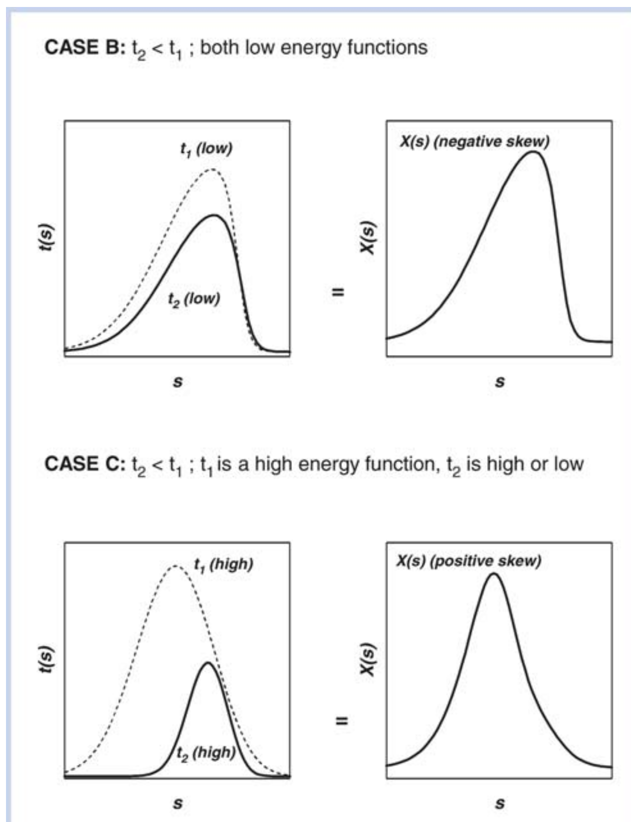

Figure A4. Summary diagram of t_1 and t_2 and corresponding X distribution (Eqn. 10b) for cases B and C (Table A1).

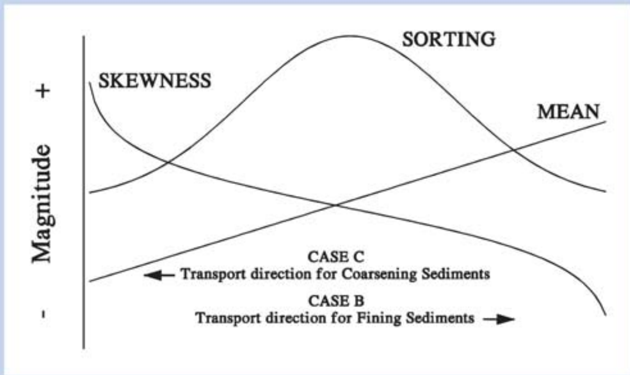

Figure A5. Changes in grain size descriptors along transport paths.

In reality, perfect sequential changes along a transport path as determined by the model and summarized in Figure A5 are rarely observed. This is because of a variety of uncertainties that can be introduced in sampling, in the analytical technique to obtain grain size distributions, in the assumptions of the transport model, and in the statistics used in describing the grain size distributions. These uncertainties are discussed in further detail (see *Uncertainties* section).

The use of the Z score statistic

One approach that appears to be successful in minimizing uncertainty is a simple statistical method whereby the case (Table A1) is determined among all possible sample pairs contained in a specified sequence. Given a sequence of n samples, $(n^2 - n)/2$ directionally orientated pairs can exhibit a transport trend in one direction and an equal number of pairs in the opposite direction. When any 2 samples are compared with respect to their distributions, the mean can become finer (F) or coarser (C), the sorting can become better (B) or poorer (P), and the skewness can become more positive (+) or more negative (–). These 3 parameters provide 8 possible combinations (Table A2).

In STA, if it is postulated that a certain relationship exists among the set of n samples and that this relationship is evidenced by particular changes in sediment size descriptors between pairs of samples, then the number of pairs for which the trend relationship occurs should exceed the number of pairs that would be expected to occur at random by a sufficient amount to state confidently that the trend relationship exists. Suppose that the probability of any trend existing between any pair of samples, if the trend relationships were established randomly, is p. Since there are 8 possible trend relationships among 3 sediment descriptors, and it is assumed that each of these is equally likely to occur, the p value is set to 0.125.

To determine whether the number of occurrences of a particular case exceeding the random probability of 0.125, the following 2 hypotheses are tested:

H_0: $p < 0.125$ with no preferred direction

H_1: $p > 0.125$ and transport occurs in the preferred direction.

With the Z score statistic in a 1-tailed test (Spiegel 1961), H_1 is accepted if

$$Z = \frac{x - Np}{\sqrt{Nqp}} > 1.645 (\text{at the } 5\% \text{ level}) \text{ or } > 2.33 (\text{at the } 1\% \text{ level}) \quad (11)$$

where x is the observed number of pairs representing a particular case in 1 of the 2 opposing directions and N is the total number of possible unidirectional pairs given by $(n^2 - n)/2$. The number of samples in the sequence is n; $p = 0.125$; and $q = 1.0 - p = 0.875$.

The Z statistic is considered valid for $N > 30$ (i.e., a large sample). Thus, for this application, a suite of 8 or 9 samples is the minimum required to evaluate a transport direction.

The use of the correlation coefficient R^2

To assess the validity of any transport line, we use the Z score and an additional statistic, the linear correlation coefficient R^2, defined as

$$R^2 = \frac{\sum_i (\hat{y}_i - \bar{y})^2}{\sum_i (y_i - \bar{y})^2}, \quad \text{where } \hat{y} = f(x_1, x_2, \ldots) \text{ and}$$

$$\bar{y} = \frac{1}{N} \sum_i y_i \quad (12)$$

The value of R^2 can range from 0 to 1. The definition of R^2 is based on the use of a model to relate a dependent parameter y to 1 or more independent parameters $(x_1, x_2, \ldots)$. In this case, the model used is linear, which can be written as

$$\hat{y} = a_o + a_1 x_1 + a_2 x_2 \quad (13)$$

The data (y, x_1, x_2) are grain size distribution statistics, and the parameters (a_0, a_1, a_2) are estimated from the data with a least squares criterion. The dependent parameter is defined as the skewness, and the independent parameters are the mean size and the sorting. An implicit assumption is made that distributions taken from samples along a transport pathway, if plotted in skewness/sorting/mean space (as in Figure A5), would tend to be clustered along a straight line. The slopes of the straight line, which are the fitted parameters, would depend on the type of transport (fining or coarsening). Although there is no theoretical reason to expect a linear relationship among the 3 descriptors, there is also no theory predicting any other kind of relationship, so according to the principle of Occam's razor, the simplest available relationship

Table A2. All possible combinations of grain size parameters

	1[a]	2	3	4	5	6	7[b]	8
Mean	F	C	F	F	C	F	C	C
Sorting	B	B	P	B	P	P	B	P
Skewness	–	–	–	+	+	+	+	–

[a] Case B trend.
[b] Case C trend.

was chosen for the model. (Occam's razor: Entities ought not to be multiplied except from necessity. Occam was a 14th Century philosopher who died in 1349.) High values of R^2 ($\geq$0.8) together with a significantly high value of the Z score provide confidence in the validity of the transport line.

A low R^2 can occur, even when the Z score statistic is acceptable. On the basis of the empirical evaluation of many sediment trend analyses from many different environments, it appears that low R^2 values can result when 1) sediments on an assumed transport path are, in reality, from different facies and valid trend statistics occurred accidentally; 2) the sediments are from a single facies, but the chosen sequence is only a poor approximation of the actual transport path; and 3) extraneous sediments have been introduced into the natural transport regime, as in the case of dredged material disposal. R^2, therefore, is assessed qualitatively and can provide extra useful information on the sediment transport regime under study.

The Z score and R^2 statistics for each of the sample sequences (Figure 4) used to determine the sediment transport patterns in the Hylebos Waterway are provided in Appendix 2.

Uncertainties

The McLaren and Bowles (1985) model requires that the grain size distributions of the sampled sediments be described in statistical terms (by the moment measures of mean, sorting, and skewness). The basic underlying assumption is that sequential deposits following the pathway of net sediment transport will affect the statistics of the particle size distributions of the sediments in a predictable way. Following from this assumption, the size frequency distributions of the sediments provide the data with which to search for patterns of net sediment transport.

Assumptions in the transport model—Whatever method is used to describe sediments, STA requires a model of the sediment transport process. The STA model is based on the assumption that smaller grains are generally more easily transported than larger grains (i.e., the probability of transport, on a phi scale, monotonically increases as grain size decreases). Under this assumption, it can be shown that erosion and deposition of sediments will change the moments of their particle size distributions in a predictable way in the direction of transport. However, as seen in transfer functions obtained from sediment data in flume experiments, this assumption might not always be strictly true. More often, the transfer function monotonically increases over only a portion of the available grain sizes before returning to 0. Furthermore, contained within the assumption is a further hidden assumption that the probability of transport of 1 particular grain size must therefore be independent of the transport of other grain sizes. Factors such as shielding, whereby the presence of larger grains can impede the transport of smaller grains; an increase in the cohesion of the finer grains; or a decrease in the ability of the eroding process to carry additional fines with increasing load all suggest that the transport process is a complicated function related to the sediment distribution and the strength of the erosion process.

Thus, the mathematics of the theory demand the somewhat unsatisfactory assertion that the probability of transport must increase monotonically over a sufficiently large range of sizes present in the deposits to produce the predicted changes. As Gao and Collins (1994) pointed out, the technique to determine net transport pathways in a wide variety of different marine and coastal environments has been empirically validated through the use of alternative approaches, indicating that such an assumption cannot be too unreasonable.

Temporal fluctuation—The particle size distribution of a particular facies can be the result of sediment arriving from several different directions and at different times. It is assumed that what is sampled is the average of all the sediment derived from an unknown number of directions. The average transport direction might not conform to that developed for a specific particle population associated with a single transport pathway.

In STA, it is assumed that a sample provides a representation of a specific sediment type (or facies) with no direct time connotation. Nor does the depth to which the sample was taken contain any significance provided that the sample does, in fact, accurately represent the facies.

Consider, for example, a beach face composed of many lamina. Each lamina might represent a particular transport and depositional event that, at a small scale, might be locally different from that of the beach transport regime as a whole. The latter can be determined by sampling the beach face in such a way that a sufficient number of lamina are incorporated into the sample to allow the assumption that the sample now represents an average of the beach face facies. The average distribution of all the lamina making up the beach face can now be compared with a similar sample taken elsewhere on the beach face. To provide another example, d_1 might be a sample representing an accumulation over several tidal cycles, whereas d_2 represents several years of deposition. The trend analysis simply determines whether a possible sediment transport relationship or pathway between the 2 deposits exists.

Sample spacing—The sampling interval might be too great (frequency too low) to detect relevant transport directions. With increasing distance between sample locations comes an increasing possibility of collecting sediments unrelated by transport. Communications theory (discussed in further detail in the *Communications analogy* section) indicates that to represent accurately a continuous signal with samples, the signal must be sampled at twice the highest frequency contained in the signal (Shannon 1948). This would imply that for STA, sample sites placed x km apart could only reliably detect transport directions occurring over a distance in the order of $2x$ km or more. Directions occurring over distances less than $2x$ km would appear as noise or could create spurious transport pathways through the process of aliasing.

In practice, selection of a suitable sample spacing must take into account 1) the number of sedimentological environments likely to affect the area under specific study, 2) the desired spatial scale of the sediment trends, and 3) the geographic shape and extent of the study area.

Random environmental and measurement uncertainties—All samples will be affected by random errors. These can include unpredictable fluctuations in the depositional environment, the effects of sampling and subsampling a representative sediment population, and random measurement errors.

Communications analogy

Sediment trend analysis is, in many ways, analogous to communications systems. In the latter, information is transmitted to a distant location, where a signal is received that includes both the desired information as well as noise. The receiver must be capable of extracting the information from the noisy signal. In sedimentary systems, the information is the transport direction and the received signal is the sediment samples. The goal of STA is to extract the information from the noisy signal. In theory, the information can be recovered by simply subtracting the noise from the signal, an approach that works well in communications systems because the nature of the information and the noise are both well known. This approach, however, will be difficult in STA because neither the nature of the information nor the noise is well understood.

A large body of analytical techniques has been developed to extract signals in communications systems. These techniques generally fall into 2 categories: Signal coding and noise reduction. For example, in FM radio transmission, the signal is coded as a time-varying frequency about a carrier frequency. At the receiver, rejecting all frequencies other than the carrier frequency reduces noise. The receiver then looks for the time-varying frequency component to extract the original signal. Reducing the noise increases the level of the signal to noise ratio, enabling the signal to be detected. Coding the signal simply makes it easier to find because of prior knowledge of the information. It is important to note that knowing what is being looked for is of critical importance in communications systems: merely analyzing the incoming signal would not be sufficient to interpret the signal correctly.

In STA, with no opportunity to code the signal, other aspects of communications theory (noise reduction) might have applications pertinent to the technique. Typically, noise in communications systems is reduced with the use of filters that selectively reduce the signal level for frequencies outside the frequency range of the signal. If these frequency components contain parts of the signal, the filter, too, will reduce them. Knowing the nature of the noise and the signal, filters can be designed that optimally increase the signal to noise ratio.

The situation in STA is not as straightforward because the noise is not well understood and the nature of the signal is only incompletely understood. In this situation, noise reduction by filtering can be problematic because the filtering can remove significant signal components; however, some statistical communications techniques might be applicable to improve the situation.

In a sedimentary system, noise can be considered in 2 areas, sample noise and spatial noise.

Sample noise—Even in a uniform sediment deposit, individual samples can be corrupted by noise. One way to address this noise would be to take many samples in close proximity and average them to produce a characteristic sample. Another method that implicitly attempts to reduce this noise is curve fitting. For example, there has been considerable research on the use of a log-hyperbolic curve to describe sediments because it appears to provide a good fit to many naturally occurring deposits (Barndorff-Nielsen 1977; Bagnold and Barndorff-Nielsen 1980). Similar to the concepts of STA, it has been shown that parameters of the log-hyperbolic distribution should change in deterministic ways under the influence of erosion or deposition (Barndorff-Nielsen and Christiansen, 1988). It was proposed that erosion and deposition cause the location shape–invariant parameters of the log-hyperbolic distribution to vary in particular ways when plotted on the shape triangle of the log-hyperbolic distribution (Barndorff-Nielsen et al. 1991; Hartmann and Christiansen 1992). Not all researchers, however, are convinced that log-hyperbolic distributions provide superior information (e.g., Wyrwoll and Smyth 1988; Hill and McLaren 2001),

Curve fitting analysis, whether log-normal or log-hyperbolic, is based on the assumption that sediments follow specific distributions. By fitting a curve to the sedimentary data, it is assumed that points that do not fall on the curve are noise and are removed. In theory, this works if in fact sediments do conform to the proposed curve. If they do not, then the curve-fitting process removes signal as well as noise; accordingly, a fitted curve could be more noisy than the original sample. In the present line-by-line approach of STA, the pitfalls of curve fitting are avoided because only the raw data of each sediment grain size distribution are used from which the log moments are calculated.

Spatial noise—As sediment is transported over a distance, noise can be introduced. To reduce this noise, average values of groups of samples could be used. Many of the techniques proposed by researchers are, in reality, efforts to reduce noise in this manner (i.e., the 1-dimensional *Z* score, as described above, or the vector approaches of Gao [1996] and Le Roux [1994]). These procedures generally involve some form of averaging of samples, which is not strictly valid. If the nature of the noise and the information is not known, the averaging of samples can reduce the information content more than it reduces the noise levels. (An exception is to reduce random noise by averaging a number of samples from the same local environment to generate a better single distribution representative of that environment.)

In STA, the assumption is that noise is randomly distributed and therefore averages to 0, leaving the true trend as the residual after averaging. Although these techniques might in fact reduce noise, signal-processing techniques might provide more refined and controllable methods.

In communications theory, it is often convenient to transform the signal from the time domain (i.e., a signal that varies over time) to the frequency domain, which shows the frequency spectrum of the signal (i.e., the amount of the signal that is carried by all of the individual frequency components). Mathematically, this is performed with a Fourier transform, which converts the signal into its frequency components. After removing the undesirable (noise) components, an inverse transform is performed to transform the signal back to the time domain. In sediment analysis, the signal varies across distance rather than time, but exactly the same analysis can be performed. In this case, the data (the grain size distributions of the sediment samples) can be represented as a sum of distance-varying sinusoids with a 2-dimensional Fourier transform. What the transform produces is a characterization of the sedimentary deposits that shows how they vary over different distance scales. For example, 1 component would indicate the intensity of changes over a 100-m range, another over a 1-km range, etc. (Note that the sample spacing, as discussed above, will set limits as to what distance ranges can be considered.) Having the signal in this form allows the unwanted components to be removed. However, how is it known what is undesirable? In communications systems, the information is known (if it was not, it would be difficult, if not impossible, to find anything). By analogy, in performing a simple analysis of the sedimentary data (e.g., mapping the variation in the mean grain size) it is highly unlikely that a transport direction would be discovered. To extract the relevant signal, it is necessary to make an assumption as to what is being looked for. It is then possible to filter the data to highlight this and detect whether in fact a signal corresponding to the assumption is actually present. For example, assume a transport process that would produce the fining of sediments over a 5-km distance. To extract this process, a 2-dimensional Fourier transform can be calculated, and all frequency components associated with variations of less than 5 km could be removed. An inverse transformation of the data would then highlight variations over the proposed distance scale.

The important feature of this approach (which, in fact, approximates the line-by-line approach discussed previously) is the use of many sample sites to detect the dominant transport direction. This effectively reduces the level of noise. The problem, however, is that it is difficult to mechanize because the number of possible transport directions in a given area can be much too large to try them all. The choosing of a trial transport direction cannot be easily analytically codified and can only be reduced to a manageable level through experience and information from other sources (e.g., bathymetric data).

In using the Z score statistic, however, a transport trend can be determined whereby all possible pairs in a sample sequence are compared with each other. When either a case B or case C trend exceeds random probability within the chosen sample sequence, the direction of net sediment transport can be inferred. As suggested before, the grid spacing must be compatible with the area under study and take into account the number of sedimentological environments likely to be involved, the geographic shape of the study area, and the desired statistical certainty of the pathways. For practical purposes, it has been found that, for regional studies in open ocean environments, sample spacing should not exceed 1 km; in estuaries, spacing can be reduced to 500 m. For site-specific studies (e.g., to determine the transport regime for a single marina), sample spacing will be reduced so that a minimum number of samples can be taken to ensure adequate coverage. Experience has also shown that extra samples should be taken over sites of specific interest (e.g., dredged material disposal sites) and those areas in which the regular grid is insufficient to accommodate specific bathymetric features (e.g., bars and channels).

At present, the line-by-line approach is undertaken as follows:

1) Assume the direction of transport over an area comprising many sample sites;
2) From this assumption, predict the sediment trends that should appear at the sample sites;
3) Compare the prediction with the Z score statistic obtained from the grain size distributions of the samples; and
4) Modify the assumed direction and repeat the comparison until the best fit is achieved.

Following from the communications analogy, when a final and coherent pattern of transport pathways is obtained that encompasses all, or nearly all, of the samples, the assumption that information (the transport pathways) is contained in the signal (the grain size distributions) has been verified, despite the inability to define accurately all the uncertainties that might be present.

It must be emphasized that the actual processes responsible for the transport of particles along the derived pathways are unknown. They might in one environment be breaking waves in a littoral drift system; in another, the residual tidal currents; and in still another, the incorporated effects of bioturbation. Nevertheless, one of the great values in obtaining the transport patterns is to assess the probable processes that are likely taking place to achieve such patterns.

INTERPRETATION OF THE *X* DISTRIBUTION

The shape of the X distribution is important in defining the type of transport (dynamic behavior of the bottom sediments) occurring along a line (erosion, accretion, total deposition, etc.); thus, the computation of X is important. Consider a transport line containing N source/deposit (d_1/d_2) pairs. X is then defined as in Equation 14.

$$X(s) = \sum_{i=1}^{N} \frac{(d_2)_i(s)}{(d_1)_i(s)} \qquad (14)$$

Often, d_2 in one pair is d_1 in another pair, and vice versa. Mean values of d_2 and d_1 are computed with Equation 15.

$$\bar{d}_1(s) = \sum_{i=1}^{N} (d_1)i(s) \qquad \bar{d}_2(s) = \sum_{i=1}^{N} (d_2)_i(s) \qquad (15)$$

Note that X is not defined as the quotient of the mean value of d_2 divided by the mean value of d_1, even though the results of the 2 computations are often almost identical. For ease of comparison, d_1, d_2, and X are normalized before plotting in reports, although there is no reason to expect that the integral of the X distribution should be unity. $X(s)$ can be thought of as a function that describes the relative probability of each particle being removed from d_1 and deposited at d_2.

Examination of X distributions from a large number of different environments has shown that 5 basic shapes are most common when compared with the distributions of the deposits $d_1(s)$ and $d_2(s)$ (Figure A6).

1. Dynamic Equilibrium—The shape of the X distributions closely resembles $d_1(s)$ and $d_2(s)$. The relative probability of grains being transported, therefore, is a similar distribution to the actual deposits. Thus, the probability of finding a particular sized grain in the deposit is equal to the probability of its transport and redeposition (i.e., there must be a grain-by-grain replacement along the transport path). The bed is neither accreting nor eroding and is, therefore, in dynamic equilibrium.

An X distribution signifying dynamic equilibrium can be found in either case B or case C transport, suggesting a fine balance between erosion and accretion. Often when such environments are determined, both case B and case C trends can be significant along the selected sample sequence. This is referred to as a "mixed case," and when this occurs, it is believed that the transport regime is also approaching a state of dynamic equilibrium.

2. Net Accretion—The shapes of the 3 distributions are similar, but the mode of X is finer than the modes of $d_1(s)$ and $d_2(s)$. The mode of X can be thought of as the size that is the most easily transported. Because the modes of the deposits are coarser than X, these sizes are more readily deposited than transported. The bed, therefore, must be in a state of net accretion. Net accretion can only be seen in case B transport.

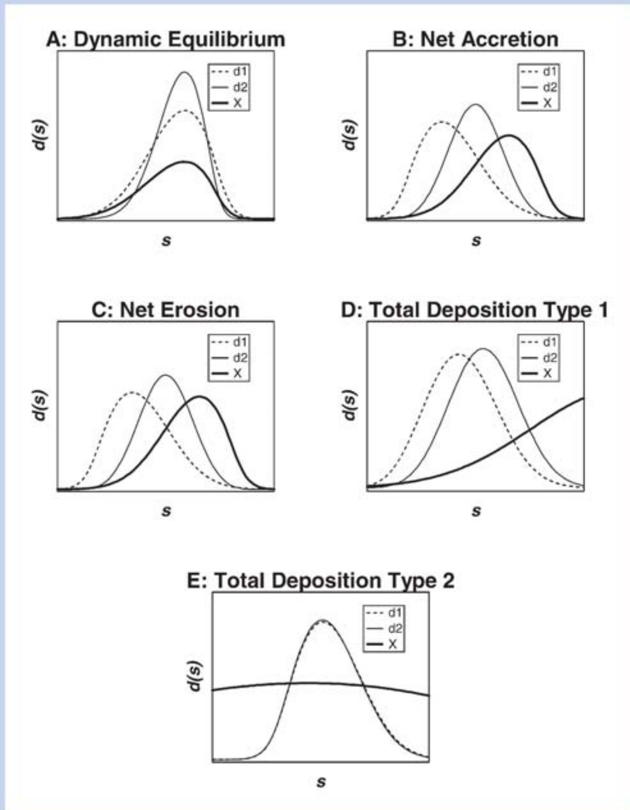

Figure A6. Summary of the interpretations given to the shapes of X distributions relative to the d_1 and d_2 deposits.

3. *Net Erosion*—Again the shapes of the 3 distributions are similar, but the mode of X is coarser than of $d_1(s)$ and $d_2(s)$. This is the reverse of net accretion; the size most easily transported is coarser than the deposits. As a result, the deposits are undergoing erosion along the transport path. Net erosion can only be seen in case C transport.

4. *Total Deposition (type 1)*—Regardless of the shapes of $d_1(s)$ and $d_2(s)$, the X distribution more or less increases monotonically over the complete size range of the deposits. Sediment must fine in the direction of transport (case B); however, the bed is no longer mobile. Rather, it is accreting under a rain of sediment that fines with distance from source. Once deposited, transport ceases. The occurrence of total deposition is usually confined to cohesive, muddy sediments.

5. *Total Deposition (type 2, horizontal X distributions)*—Occurring only in fine sediments when the mean grain size is a very fine silt or clay, the X distribution can be essentially horizontal. Such sediments are usually found far from their source, and the horizontal nature of the X distribution suggests that their deposition is no longer related strictly to size sorting. In other words, all sizes now have an equal probability of being deposited. This form of the X distribution was 1st observed in the muddy deposits of a British Columbia fjord and is described in McLaren et al. (1993). Because the trends occur in very fine sediments, in which any changes in the distributions are extremely small, horizontal X distributions can be found in both case B and case C trends.

REFERENCES

Bagnold RA, Barndorff-Nielsen OE. 1980. The pattern of natural size distributions. *Sedimentology* 27:199–207.

Barndorff-Nielsen OE. 1977. Exponentially decreasing distributions for the logarithm of particle size. *Proc R Soc Lond A* 353:401–419.

Barndorff-Nielsen OE, Christiansen C. 1988. Erosion, deposition and size distributions of sand. *Proc R Soc Lond, A* 417:335–352.

Barndorff-Nielsen OE, Christiansen C, Hartmann D. 1991. Distributional shape triangles with some applications in sedimentology. *Acta Mechanica* 2:37–47.

Bowles D, McLaren P. 1985. Optimal configuration and information content of sets of frequency distributions—Discussion. *J Sediment Petrol* 55:931–933.

Gao S. 1996. A Fortran program for grain-size trend analysis to define net sediment transport pathways. *Comput Geosci* 22:449–452.

Gao S, Collins M. 1994. Analysis of grain size trends, for defining sediment transport pathways in marine environments. *J Coast Res* 10:70–78.

Hartmann D, Christiansen C. 1992. The hyperbolic shape triangle as a tool for discriminating populations of sediment samples of closely connected origin. *Sedimentology* 39:697–708.

Hill SH, McLaren P. 2001. A comparison between log-hyperbolic and model independent grain size distributions in Sediment Trend Analysis. *J Coast Res* 17:931–935.

Le Roux JP. 1994. An alternative approach to the identification of net sediment transport paths based on grain-size trends. *Sediment Geol* 94:97–107.

McLaren P. 1981. An interpretation of trends in grain-size measures. *J Sediment Petrol* 51:611–624.

McLaren P, Bowles D. 1985. The effects of sediment transport on grain-size distributions. *J Sediment Petrol* 55:457–470.

McLaren P, Cretney WJ, Powys R. 1993. Sediment pathways in a British Columbia fjord and their relationship with particle-associated contaminants. *J Coast Res* 9:1026–1043.

Shannon CE. 1948. A mathematical theory of communication. *Bell Syst Technol J 27:379–423,* 623–656.

Spiegel MA. 1961. Theory and problems of statistics. New York (NY): McGraw-Hill. 379 p.

Wyrwoll KH, Smyth GK. 1988. On using the log-hyperbolic distribution to describe the textural characteristics of eolian sediments. *J Sediment Petrol* 55:471–478.

Appendix 2

SEDIMENT TREND STATISTICS FOR ALL SELECTED SAMPLE LINES (SEE FIGURE 4)

Definitions:

1) R^2 is the multiple correlation coefficient derived from the mean, sorting, and skewness of each sample pair making up a significant trend. This is a relative indication of how well the samples are related by transport.
2) Case B: Sediments becoming finer, better sorted, and more negatively skewed in the direction of transport.
3) Case C: Sediments becoming coarser, better sorted, and more positively skewed in the direction of transport.
4) N is the number of possible pairs in the line of samples.
5) X is the number of pairs making a particular trend in a specific direction.
6) Z is the Z score statistic. Only trends at the 99% level are accepted.
7) "Down" indicates transport in the down-line direction. "Up" indicates transport in the up-line direction.
8) Status defines the dynamic behavior of the sediments making up the line of samples (i.e., Net Erosion, Net Accretion, Dynamic Equilibrium, etc.) See Appendix 1 for a complete explanation.

Line Nr[a]	Case	Direction	R^2	*N*	*X*	Z^b	Interpretation of dynamic behavior
1	B	Down	1	6	4	4.01**	Total Deposition (type 1)
		Up		6	1	0.31	
	C	Down		6	0	−0.93	
		Up		6	1	0.31	
2	B	Down	1	15	11	7.12**	Total Deposition (type 1)
		Up		15	3	0.88	
	C	Down		15	0	−1.46	
		Up		15	1	−0.68	
3	B	Down	0.99	15	8	4.78**	Total Deposition (type 1)
		Up		15	3	0.88	
	C	Down		15	0	−1.46	
		Up		15	2	0.1	
4	B	Down	0.99	21	13	6.85**	Total Deposition (type 1)
		Up		21	2	−0.41	
	C	Down		21	3	0.25	
		Up		21	0	−1.73	
5	B	Down	0.98	36	22	8.82**	Total Deposition (type 1) (see Figure 7)
		Up		36	7	1.26	
	C	Down		36	3	−0.76	
		Up		36	1	−1.76	
6	B	Down	0.3	15	2	0.1	Net Erosion
		Up		15	1	−0.68	
	C	Down		15	5	2.44**	
		Up		15	3	0.88	
7	B	Down	0.95	21	0	−1.73	Net Erosion (see Figure 6)
		Up		21	4	0.91	
	C	Down		21	11	5.53**	
		Up		21	3	0.25	
8	B	Down	0.94	21	0	−1.73	Net Erosion
		Up		21	3	0.25	
	C	Down		21	8	3.55**	
		Up		21	6	2.23*	
9	B	Down	0.7	15	7	4.00**	Net Accretion
		Up		15	0	−1.46	
	C	Down		15	4	1.66*	
		Up		15	0	−1.46	
10	B	Down	1	3	2	2.84**	Net Accretion
		Up		3	0	−0.65	
	C	Down		3	0	−0.65	
		Up		3	0	−0.65	

Continued.

Line Nr[a]	Case	Direction	R^2	*N*	*X*	Z^b	Interpretation of dynamic behavior
11	B	Down	0.95	45	31	11.44**	Dynamic Equilibrium
		Up		45	5	−0.28	
	C	Down		45	2	−1.63	
		Up		45	4	−0.73	
12	B	Down		36	9	2.27*	Dynamic Equilibrium
		Up		36	3	−0.76	
	C	Down	0.89	36	16	5.80**	
		Up		36	3	−0.76	
13	B	Down		55	8	0.46	Net Erosion
		Up		55	5	−0.76	
	C	Down	0.93	55	33	10.65**	
		Up		55	3	−1.58	
14	B	Down	0.95	91	24	4.00**	Mixed case
		Up		91	8	−1.07	
	C	Down	0.94	91	33	6.85**	
		Up		91	14	0.83	
15	B	Down	0.93	120	34	5.24**	Mixed case
		Up		120	23	2.21*	
	C	Down	0.97	120	42	7.45**	
		Up		120	10	−1.38	
16	B	Down	0.98	66	38	11.07**	Dynamic Equilibrium
		Up		66	8	−0.09	
	C	Down		66	1	−2.7	
		Up		66	4	−1.58	
17	B	Down	0.98	66	32	8.84**	Dynamic Equilibrium (see Figure 8)
		Up		66	10	0.65	
	C	Down		66	2	−2.33	
		Up		66	6	−0.84	
18	B	Down	0.98	55	32	10.24**	Total Deposition (type 1)
		Up		55	9	0.87	
	C	Down		55	6	−0.36	
		Up		55	5	−0.76	
19	B	Down	0.97	28	12	4.86**	Dynamic Equilibrium
		Up		28	2	−0.86	
	C	Down		28	7	2.00*	
		Up		28	4	0.29	
20	B	Down	0.99	28	4	0.29	Net Erosion
		Up		28	5	0.86	
	C	Down		28	13	5.43**	
		Up		28	3	−0.29	

Continued.

Line Nr[a]	Case	Direction	R^2	*N*	*X*	Z^b	Interpretation of dynamic behavior
21	B	Down	1	36	6	0.76	Net Erosion
		Up		36	3	−0.76	
	C	Down		36	19	7.31**	
		Up		36	4	−0.25	
22	B	Down	0.91	28	13	5.43**	Total Deposition (type 1)
		Up		28	5	0.86	
	C	Down		28	2	−0.86	
		Up		28	2	−0.86	
23	B	Down	0.88	28	18	8.29**	Total Deposition (type 1)
		Up		28	2	−0.86	
	C	Down		28	0	−2	
		Up		28	2	−0.86	
24	B	Down	0.85	36	19	7.31**	Total Deposition (type 1)
		Up		36	2	−1.26	
	C	Down		36	0	−2.27	
		Up		36	2	−1.26	
25	B	Down	0.98	66	34	9.58**	Total Deposition (type 1) (see Figure 9)
		Up		66	2	−2.33	
	C	Down		66	0	−3.07	
		Up		66	11	1.02	
26	B	Down	0.99	55	34	12.69**	Total Deposition (type 1)
		Up		55	4	−1.17	
	C	Down		55	6	−0.36	
		Up		55	2	−1.99	
27	B	Down	0.88	55	20	5.35**	Total Deposition (type 1)
		Up		55	9	0.87	
	C	Down		55	8	0.46	
		Up		55	4	−1.17	
28	B	Down	0.71	78	23	4.54**	Total Deposition (type 2)
		Up		78	14	1.46	
	C	Down		78	5	−1.63	
		Up		78	1	−3	
29	B	Down	0.74	91	38	8.44**	Total Deposition (type 2) (see Figure 10)
		Up		91	7	−1.39	
	C	Down		91	3	−2.65	
		Up		91	6	−1.7	
30	B	Down	0.7	78	39	10.01**	Total Deposition (type 2)
		Up		78	6	−1.28	
	C	Down		78	3	−2.31	
		Up		78	2	−2.65	

Continued.

Line Nr[a]	Case	Direction	R^2	N	X	Z^b	Interpretation of dynamic behavior
31	B	Down	0.75	120	53	10.49**	Total Deposition (type 2)
		Up		120	9	−1.66	
	C	Down		120	7	−2.21	
		Up		120	12	−0.83	
32	B	Down	0.97	45	19	6.03**	Total Deposition (type 2)
		Up		45	8	1.07	
	C	Down		45	7	0.62	
		Up		45	5	−0.28	
33	B	Down	0.93	210	65	8.09**	Total Deposition (type 2)
		Up		210	35	1.83*	
	C	Down		210	19	−1.51	
		Up		210	20	−1.3	
34	B	Down	0.93	66	29	7.72**	Total Deposition (type 2)
		Up		66	14	2.14*	
	C	Down		66	10	0.65	
		Up		66	2	−2.33	
35	B	Down	1	6	0	−0.93	Dynamic Equilibrium
		Up		6	0	−0.93	
	C	Down		6	3	2.78**	
		Up		6	2	1.54	

[a] See Figure 4.
[b] Trends are significant at the * 95% and ** 99% level.